Stepwise progression of β-selection during T cell development as revealed by histone deacetylation inhibition

A histone deacetylase 6 inhibitor disrupts early αβ T cell development

[1,2,8]Anchi S Chann, [1,2,8]Mirren Charnley, [3]Lucas Newton, [7,8]Andrea Newbold , [3,4,5,6]Patrick O Humbert, [7,8]Ricky W Johnstone, [1,2,7,8]Sarah M Russell.

Affiliations

[1]Optical Sciences Centre, School of Science, Swinburne University of Technology, Hawthorn, Victoria 3122; Australia.

[2]Immune Signalling Laboratory, Peter MacCallum Cancer Centre, Melbourne, Victoria 3000 Australia.

[3] Department of Biochemistry & Genetics, La Trobe Institute for Molecular Science, La Trobe University, Melbourne, Victoria 3086, Australia.

[4] Research Centre for Molecular Cancer Prevention, La Trobe University, Melbourne, Victoria 3086, Australia.

[5] Department of Biochemistry & Molecular Biology, University of Melbourne, Melbourne, Victoria 3010, Australia.

[6] Department of Clinical Pathology, University of Melbourne, Melbourne, Victoria 3010, Australia.

[7]Sir Peter MacCallum Department of Oncology, The University of Melbourne, Victoria 3010, Australia.

[8]Peter MacCallum Cancer Centre, Melbourne, Victoria 3000, Australia.

*To whom correspondence should be addressed: Sarah Russell: sarah.russell@petermac.org; 613-433-354-996; Optical Sciences Centre, School of Science, Hawthorn, Australia

ORCID ID: 0000-0002-8778-5327 (ASC); 0000-0003-3845-9290 (MC); 0000-0002-0481-2431 (AN); 0000-0002-1366-6691(POH); 0000-0001-7053-9237 (RWJ); 0000-0001-5826-9641 (SMR);

Abstract

During T cell development, the first step in creating a unique T Cell Receptor (TCR) is the genetic recombination of the TCRβ chain. The quality of this newly recombined gene is assessed at the β-selection checkpoint, and most cells fail this checkpoint and are removed. The coordination of the complex events that combine to control fate at the β-selection checkpoint is not yet understood. We assessed the impact on T cell development of a selective inhibitor to histone deacetylase 6, ACY1215, currently in clinical use. ACY1215 led to bypass of the β-selection checkpoint such that cells in the DN4 stage often lacked expression of TCRβ, and failed to progress to the DP stage. Characterisation of the molecular basis for this bypass revealed a new, pivotal stage in β-selection, the beginning and end of which were defined by the upregulation of the TCR co-receptors, CD28 and CD2 respectively. Within this stage, termed DN3b^{Pre}, CD5 and Lef1 are upregulated to reflect pre-TCR signalling. We propose that the progressive expression of CD28, CD5 then CD2 reports and modulates the pre-TCR signal to orchestrate passage through the β-selection checkpoint. By disrupting the functional connection between CD5 and pre-TCR, ACY1215 allows cells to inappropriately bypass the β-selection checkpoint. These findings implicate a refined model of β-selection in which a coordinated increase in expression of pre-TCR, CD5 and Lef1 provides for an escalating test of TCR signalling strength, and culminates in the expression of CD2 to enable exit from the β-selection checkpoint.

Introduction

T cells are generated in a multistep, highly orchestrated process guided by stromal cells in the thymus. T cell development involves massive cell proliferation interspersed with genomic recombination of the T cell receptor (TCR). If genomic recombination, proliferation and death are not appropriately orchestrated, the implications for cancer and immunity are profound. Uncontrolled self-renewal or a sub-optimal TCR repertoire can lead to T cell acute lymphoblastic lymphoma (T-ALL), autoimmunity or limited response to pathogens or cancers (Ballesteros-Arias et al., 2019; Douek et al., 2000; Notarangelo et al., 2020). T cell development is particularly tightly controlled during genomic recombination to generate the TCR. For αβ T cells, a major branch of adaptive immunity, the β chain is generated at the DN3a phase of T cell development (see **Fig 1A** for a description of T cell

development and how it is assessed), and the appropriateness of this TCRβ sequence is assessed by a process termed the β-selection checkpoint. During β-selection, the strength of the TCRβ chain is tested in combination with a surrogate 'pre-TCR' before the TCRα chain is created (Chann and Russell, 2019; Dutta et al., 2021).

β-selection is in part determined by stromal cells in the thymic microenvironment, which provide Notch and chemokine signals that promote survival and differentiation (Chann and Russell, 2019; Dutta et al., 2021). Recently, it has become clear that interactions between the pre-TCR and the MHC-peptide on stromal cells also provides an opportunity to test TCR signalling (Allam et al., 2021; Dutta et al., 2021; Li et al., 2021) These interactions trigger a sequence of transcriptional changes and epigenetic modifications that ensure only the cells with an appropriately recombined TCRβ chain survive, proliferate and differentiate. How pre-TCR signalling integrates fate determination including proliferation, differentiation and survival during β-selection is still not understood (Chann and Russell, 2019; Dutta et al., 2021).

Epigenetic therapies such as small-molecule inhibitors of histone deacetylases (HDAC) have shown great promise in mediating clinical antitumor responses, and are also evolving as a possible means of promoting immunity to cancer (Hogg et al., 2020). A deeper understanding of the impact of histone deacetylation on both tumour control and immune regulation is therefore a topic of increasing interest (Hogg et al., 2020).The HDAC6 selective inhibitor ACY1215 (Ricolinostat) can synergize with the BET inhibitor, JQ1, to recruit T cell mediated responses to lung adenocarcinoma, enhance T cell responses to *ex vivo* melanoma cultures, impair effector CD8 T cell function during skin inflammation, and alter Treg function (Adeegbe et al., 2017). (Laino et al., 2019; Tsuji et al., 2015; Xu et al., 2018; Zhang et al., 2021). HDACs 1, 2, and 3 are required at multiple stages of T cell development, but a role for HDAC6 in T cell development has not been identified (Wang et al., 2020). Mice lacking HDAC6 showed no overt T cell phenotypes (Shapiro and Shapiro, 2020; Zhang et al., 2008) and to our knowledge the effect of acute deletion of HDAC6, or pharmacological inhibition of HDAC6 on T cell development has not been reported (Shapiro and Shapiro, 2020).

Here, we show a striking effect of treatment with the HDAC6-selective inhibitor, ACY1215, on β-selection. This effect allowed us to define several stages of β-selection with high resolution. First, after the DN3a stage marked by upregulation of the co-receptor, CD28, we observed a transitional stage marked by low levels of the co-receptor, CD2, that we termed DN3b^{Pre}. DN3b^{Pre} cells are enriched by ACY1215 treatment. An upregulation of CD2 marks passage through the β-selection checkpoint, to a phase we termed DN3b^{Post}. Second, we show that the transcription factor, Lef1 is upregulated in DN3b^{Pre} cells, together with an increasing expression of the reporter and tuner of TCR signalling, CD5. Treatment with ACY1215 disrupts the functional association between pre-TCR signalling, CD5 and proliferation, enabling cells without TCRβ expression to bypass the β-selection checkpoint, and disrupting T cell development.

Results

Treatment with ACY1215 impairs T cell differentiation at the DN3 stage.

To examine whether HDAC6 inhibition influences T cell development, we used a well validated *in vitro* model in which hematopoietic stem cells extracted from mouse fetal liver were co-cultured with the OP9 mouse bone marrow stromal cell line transfected with the Notch ligand, DL1 ('OP9-DL1'). At Day 8-10 of the co-culture, when the cells were predominantly at the DN3 stage of T cell development **(**Protocol 1 in **Supp Fig 1**), we applied the HDAC6 inhibitor, ACY1215 at a concentration previously reported to have no impact on lymphocyte viability but that altered function of mature T cells (Laino et al., 2019) (**Figure 1B**). Compared with DMSO treated cells, cells treated with ACY1215 for two days (Figure 1Bi) showed an increased proportion of DN cells, and reduced proportions of the later stages of differentiation: DP, CD4-SP and CD8-SP, suggesting HDAC6 is required for optimal T cell development to the DP stage. This shift in differentiation stages was accompanied by a generalised inhibition of expansion in cell numbers at several stages of T cell development (**Supp Fig 2**). We analysed CD25 and CD44 expression in the DN cells to compare proportions at different DN stages (Figure 1Bii). An increase in the proportions of DN3 cells, and a

commensurate decrease in proportions of DN4, suggested that the ACY1215-treated cells were blocked at the DN3 stage.

To confirm that the block was at the β-selection stage, we monitored cell expansion and differentiation from DN3b that had been treated for four days with ACY1215 or DMSO (Protocol 2 illustrated in Supp Fig 1A). By day 4, approximately 25% of the control DN3b cells had progressed to DP (**Figure 1Ci**) and this proportion was reduced to below 5% by ACY1215 treatment. In addition, the relative proportions of cells within DN was biased towards DN3 rather than DN4 by ACY1215 treatment (Fig 1Cii). We performed a parallel analysis using DN3a cells as a starting population (Supp Fig 2). Although the very few DN3a cells had progressed beyond the DN stage by day 4, ACY1215 treatment led to a similar inhibition of progression from DN3a to DP. (Supp Fig 2**).** These data indicate that the major effect of ACY1215 was on the DN3b stage, but did not exclude an additional effect on DN3a cells. To determine whether the shift in proportions indicated alterations in differentiation or proliferation of particular subsets, we assessed the number of cells at each differentiation stage that developed from the sorted DN3b (Figure 1Ciii). By day 4, DN3b cells had expanded more than 50 fold, with a negligible reduction caused by treatment ACY1215. DN4 cell numbers were also only slightly reduced by ACY1215 treatment. The most dramatic effect occurred at the DP stage, with a reduction in cell number of over two orders of magnitude. Together, these data indicate that ACY1215 treatment substantially inhibited cells from progressing beyond the DN3b.

ACY1215 disrupts β-selection.

Two T cell lineages arise from DN3 cells, each expressing a different set of T cell receptors (αβ cells and γδ cells)(Hayday and Pennington, 2007). To determine which lineage was altered by ACY1215, we cultured developing T cells for 2 days with and without HDAC6i, and labelled the cells with antibodies specific for these TCRs (**Figure 2A**). As expected DN3a cells (which have not undergone genomic rearrangement) expressed neither TCRβ nor TCRγδ. As they progressed through DN3b and DN4 stages, untreated cells showed increasing proportions of cells expressing either TCRβ or TCRγδ. By the DP stage, cells predominantly expressed TCRβ as expected. ACY1215 treatment increased the proportion of cells expressing TCR away from TCRβ and towards TCRδ, with a reduced proportion

of TCRβ–expressing cells at all stages following β-selection. These data are compatible with a specific effect on TCRβ selection. To confirm the impact of ACY1215 at the β-selection stage differentiation and TCRβ and TCRγδ expression was assessed on a pure population of DN3b cells (**Figure 2B**). After 2 days of culture, alongside a general reduction in numbers of DP cells as shown in Fig 1, the number of cells expressing TCRβ was reduced significantly at DN3, DN4 and DP stages. The number of cells expressing TCRγδ was not substantially reduced by ACY1215 treatment. TCRβ^{-} cells showed a small but statistically significant decrease in number at both the DN3 and DN4 stage which might reflect an impact of ACY1215 before the cells had completed β-selection, or might merely reflect TCRβ expression below the level of detection. We confirmed these results with staining for icTCRβ (**Figure 2C**), which was expressed on fewer cells at the DN3, DN4 and DP stage by 4 days of ACY1215 treatment. Together, these data indicated that the defect in differentiation to DP following ACY1215 treatment was specific to αβ T cells, and likely involved the β-selection checkpoint.

The passing of the β-selection checkpoint is associated with progression from the DN3a to DN3b stages of differentiation, which is generally defined by expression of CD28 (**Supp Fig 3)**(Teague et al., 2010; Williams et al., 2005). We therefore assessed whether DN3a cells were inhibited from progressing to DN3b by ACY1215 treatment (**Figure 3A**). Surprisingly, the reverse was observed. In DMSO control cultures, co-staining with CD25 and CD28 indicated a relatively stable distribution between DN3a (CD28^{Lo}) and CD3b (CD28^{Hi}) at 1 and 2 days, but increasingly greater proportions of CD28^{Hi}in the ACY1215-treated cells. The conversion from predominantly DN3a in the DMSO-treated cells to predominantly DN3b in the ACY1215-treated cells could reflect either (or both) a reduction in the number of DN3a cells, or an increase in number of DN3b cells, so we calculated total cell numbers in cultures of sorted DN3a cell to address this. The DN3a cells expanded more than 4-fold over 2 days of control DMSO-treated culture. A small fraction of these cells had converted to DN3b cells after 1 day, and both DN3a and DN3b numbers increased substantially in the second day of culture. In contrast, treatment with ACY1215 reduced the number of DN3a cells on Days 1 and 2. The number of DN3b cells produced was not compromised by ACY1215 treatment, and the number

of DN4 cells was increased slightly at 1 day of treatment, but this difference was not sustained at 2 days. Together, these data suggest that ACY1215 treatment of DN3a cells led to a dramatic reduction in DN3a amplification, but little impact upon the number of cells passing through the DN3bb stage.

A caveat to the characterisation of DN3a to DN3b progression described above is that CD28 levels do not cleanly demarcate DN3a and DN3b populations. The $CD28^{Hi}$cells expressed more of the nutrient transporters, CD71 and CD98, and more surface TCRβ (**Supp Fig 4**) indicating that, in general, they had progressed further through β-selection, but the correlation was not absolute. To address this we first co-stained DN3 cells with both CD28 and CD27, both of which can discriminate between DN3a and DN3b cells (Taghon et al., 2006; Teague et al., 2010)(**Figure 3B**). This staining strategy clearly discriminated two subpopulations in DN3 cells that had been pre-treated with DMSO, with 50-60% of the population in the $CD27^{Lo}CD28^{Lo}$fraction that we classified as DN3a, similar to our finding with CD28 alone (Fig 3A). Interestingly co-staining for CD27 and CD28 did not discriminate two populations in the ACY1215-treated sample. Cell counts (based upon gating according to the two populations observed in control treatments) again showed an expansion over time of DN3a cells in the control-treated cells. Combined staining with the two markers suggested that the DN3a population was substantially depleted by ACY1215 treatment. As in Fig 3A, the numbers of $CD28^{Hi}$cells were similar in DMSO and ACY1215 cells. These data confirm that ACY1215 causes the DN3a population to contract, and indicate that normal numbers of ACY1215-treated cells differentiate to DN3b.

The reduced numbers of DN3a cells reflects a general impact of ACY1215 on proliferation.

To account for the reduced numbers of DN3a cells, DN3a cells must either die more frequently, undergo fewer cell divisions, or differentiate into non-DN3a cells. To assess whether the reduction was due to cell death, we stained the cells at 3 and 6 hours post treatment with propidium iodide (PI)(**Figure 3C**). No differences in cell death was apparent in either DN3a or DN3b cells with ACY1215 compared with DMSO, although the control DP population showed a striking increase in apoptotic cells upon ACY1215 treatment, as did DN3a and DN3b in a control sample without stromal support (Ciofani and Zuniga-Pflucker, 2005) (**Supp Fig 4**). Similar results were obtained with Annexin V labelling **(Supp Fig 4**). Despite clear induction of apoptosis in both DN3a and DN3b cells

upon withdrawal of OP9-DL1 cells, we saw no significant apoptosis in the sorted DN3a and DN3b cells after ACY1215 treatment

An alternative explanation for the reduced numbers of DN3a cells is changes in proliferation. This was confirmed with CFSE labelling. We labelled sorted DN3a and DN3b with the fluorescent dye, CFSE, and assessed dilution of the dye as an indicator of the number of cell divisions in the 2 days since labelling (**Figure 3D**). CFSE in thymocytes does not allow for precise allocation of cell divisions that can be achieved with mature T cells, but nonetheless provides a useful comparator between samples. DN3a cells showed extensive cell proliferation as indicated by a substantial reduction in CFSE labelling over 2 days, and this proliferation was clearly reduced by ACY1215 treatment. The purified DN3b cells showed greater proliferation than DN3a cells as expected, which was again substantially reduced by HDAC6i treatment.

Labelling with the marker of proliferation, Ki-67(Gerdes et al., 1984), one day after treatment showed several interesting findings (**Figure 3E**). First, the relative proportion of cells in the FSC^{Hi}Ki-67^{Hi}quadrants (which presumably reflected cells in mitosis) was substantially higher for DN3b than DN3a cells, supporting their greater proliferative rate. Interestingly, of the smaller (low FSC) cells, the Ki-67 staining was much weaker in the presence of ACY1215, suggesting a longer time since their last cell division (Miller et al., 2018). This reduced Ki67 staining was observed in both DN3a and DN3b cells, but was particularly striking for DN3a cells treated with AY1215. Thus, the reduction in DN3 cell number induced by HDAC6i treatment is at least in part due to direct effects on proliferation of DN3a cells. To assess whether the reduced proliferation of DN3a cells was stage-specific, we sorted DN2, DN3a, DN3b and DP cells, and cultured for 2 days in DMSO or ACY1215, then assessed their expansion (**Supp Fig 2B).** All four cell populations showed reduced expansion in the presence of ACY1215, suggesting that this reflects a general inhibition of proliferation, rather than an effect specific to the DN3a stage. Another possible explanation for the reduced DN3a numbers is a precocious differentiation of DN3a to DN3b. This is not easy to measure at the population level, but the observation that DN3b cell numbers are maintained despite a reduction in their proliferation is compatible with the notion that DN3a cells precociously differentiate to DN3b. Together, these data

suggest that the cellular basis for reduced DN3a cell numbers upon ACY1215 treatment is caused by reduced proliferation, perhaps precocious differentiation to DN3b, but probably not increased cell death.

ACY1215 leads to phenotypically aberrant DN3b cells

To more precisely define the DN3b cells induced by ACY1215, we first characterised several phenotypic markers that have been implicated in progression through the β-selection checkpoint. Given that the primary function of this checkpoint is to ensure appropriate TCRβ rearrangement, we assessed the correlation of each marker with TCRβ expression (**Figure 4A**). As previously shown (Williams et al., 2005), expression of CD28 was clearly correlated with expression of icTCRβ, and this correlation was not impacted by treatment with ACY1215. Similarly, expression of CD27 was increased with icTCRβ, although not all $CD27^{Hi}$cells expressed icTCRβ. Again, the association of CD27 and icTCRβ was not affected by ACY12115.

CD5 is an established reporter of the strength of TCR signalling (Voisinne et al., 2018). A role for CD5 has not been established during β-selection, but during positive selection expression of CD5 reports the strength of TCR signalling and tunes TCR signalling responsiveness, dampening the response of cells to TCR-signalling via the NF-κB pathway (Azzam et al., 2001; Azzam et al., 1998; Tarakhovsky et al., 1995). Plotting CD28 against CD5 (**Figure 4B**) showed that CD5 exhibited a wide range of expression, with the cells brightest for CD5 residing only in the DN3b population, commensurate with the notion that $CD5^{Hi}$cells have been exposed to strong TCRβ signals. To more precisely define the pattern of CD5 expression, we cultured DN3a or DN3b cells in the presence of ACY1215 or DMSO for 2 days, gated for DN3b cells, and compared CD5 expression with icTCRβ (Figure 4B). Cells from the DN3a starting population were more likely to be dull for both CD5 and icTCRβ, compared with the more mature cells from the DN3b starting population. Expression of CD5 correlated with expression of icTCRβ, suggesting that, as in other cell types, CD5 is a reporter of TCR signalling during β-selection. However, in ACY1215 cells, expression of icTCRβ was uncoupled from CD5 (**Figure 4C),** with only 15 % of $icTCR\beta^{Hi}$ cells exhibiting high levels of CD5 compared with 60 % in DMSO-treated cells. This disconnect between TCRβ and markers of successful

progression, not observed with CD27 and CD28 (Figure 4A), indicated that CD5 is specifically affected by ACY1215.

To assess the functional relevance of this disconnect between TCRβ and CD5, we compared the relationship between CD5 expression and proliferation in the presence and absence of ACY1215 (**Figure 4D**). High expression of CD5 positively correlated with proliferation in DN3b cells, and, although the extent of both proliferation and CD5 expression was reduced, this correlation was maintained in the presence of ACY1215. Thus, in the presence of ACY1215, the functional connections between TCRβ expression, CD5 upregulation, and control of proliferation are deregulated, with proliferation correlating with expression of CD5, despite the fact that expression of CD5 is no longer coupled to expression of TCRβ. These findings indicate that the cells marked as DN3b by CD27 and CD28, are not canonical DN3b cells in that the functional relationship between CD5 and TCRβ is disrupted. Given the role of CD5 in dampening a TCR response, one possible implication of this finding is that a block in CD5 upregulation induced by ACY1215 might lead to a failure of TCR tuning in these cells and allow them to progress inappropriately to the DN4 stage. This could explain the reduced TCRβ expression observed in DN4 and DP cells, and could also set the cells up to fail positive selection, explaining the loss of DP cells. Together, these data indicate that the $CD28^{Hi}$cells in ACY1215-treated cultures share some phenotypic similarities to *bone fide* DN3b cells, but express less CD5 in $TCR\beta^{+}$ cells.

CD2 expression separates DN3b into two functionally distinct populations.

Another well-established co-stimulator of TCR signalling is CD2 (Skånland et al., 2014). Expression of CD2 marks TCRβ V(D)J rearrangement and can facilitate pre-TCR signalling for passage through the β-selection checkpoint (Groettrup et al., 1992; Rodewald et al., 1993; Sasada and Reinherz, 2001). Co-staining of DMSO-treated DN3 cells with CD28 and CD2 showed that all DN3a cells ($CD28^{Lo}$) were $CD2^{Lo}$, but DN3b ($CD28^{Hi}$) cells had two clearly discernible populations of $CD2^{Lo}$and $CD2^{Hi}$(**Figure 5Ai**). The enrichment of $CD2^{Hi}$cells within the $CD28^{Hi}$population is consistent with the notion that CD2 marks cells that have achieved TCRβ V(D)J rearrangement. We therefore speculated that the two populations represented successive stages of differentiation, and tentatively termed the

two populations DN3b^{Pre} (CD28^{Hi}CD2^{Lo}) and DN3b^{Post} (CD28^{Hi}CD2^{Hi}). ACY1215 treatment enriched for the DN3b^{Pre} population, causing the CD28^{Hi}cells to skew towards CD2^{Lo}. Quantification of cell numbers indicated that the numbers of DN3b^{Pre} cells were not substantially affected by ACY1215, but DN3a and DN3b^{Post} numbers were dramatically reduced. Thus, in contrast to other stages in T cell development (**Supp Fig 2B**), the number of DN3b^{Pre} cells was not reduced by ACY1215.

To confirm that DN3b^{Post} cells represented a more differentiated state than DN3b^{Pre}, we assessed the association of CD2 expression with icTCRβ expression and Ki-67 (**Figure 5B**). Indeed, consistent with previous findings that TCRβ V(D)J recombination is restricted to DN cells positive for CD2 (Rodewald et al., 1993), CD2^{Hi}cells showed increased expression of icTCRβ and Ki-67. Given the established relationship between CD2 and pre-TCR expression and signalling, we compared the expression of TCRβ in the DN3a and the two DN3b populations (Figure 5B). As expected, DN3a cells showed minimal staining for intracellular TCRβ and for Ki-67. DN3b^{Pre} cells showed a broad spectrum of staining, with a minority population that was bright for both markers. DN3b^{Post} cells were uniformly bright for both TCRβ and Ki-67. ACY1215 treatment led to only small shifts in the expression of icTCRβ in each population, and clearer reduction of Ki-67 in each population. In accord with the Ki-67 result, CD2-stained cells that had been previously labelled with CFSE showed two clear populations, with the CD2^{Hi}(DN3b^{Post}) cells having undergone substantially more proliferation than the CD2^{Lo}(DN3b^{Pre}) cells (Fig 5C). ACY1215 treatment did not disrupt the association between CD2 and proliferation.

The transcription factor c-Myc is key to cell growth and is progressively upregulated during β-selection (Carr et al., 2015; Hao et al., 2019). We therefore assessed how c-Myc expression changed in the different β-selection stages (**Figure 5D**). Indeed, c-Myc expression steadily increased as cells progressed from DN3a to DN3b^{Pre} to DN3b^{Post}. c-Myc expression was slightly down-regulated at all stages by ACY1215 treatment, compatible with a generalised impact of the drug on cell growth. Together these results suggest that ACY1215 leads to reduction in a subpopulation of DN3b cells that are characterised by high proliferation, high CD2 expression, and high TCRβ expression (DN3b^{Post} cells). The reduction in DN3b^{Post} cells caused by ACY1215 treatment revealed a DN3b^{Pre} population

that is usually not readily discernible; characterised by moderate proliferation, and moderate expression of CD2, c-Myc and TCRβ.

The CD28^{Hi}CD2^{Lo}(DN3b^{Pre}) cells are precursors of CD28^{Hi}CD2^{Lo}(DN3b^{Post})

To assess whether the DN3b^{Pre} stage was a transitional stage before DN3b^{Post}, we sorted DN3a, DN3b^{Pre} and DN3b^{Post} cells and cultured them for further analysis. Cells were sorted from both ACY1215 treated and untreated cells to take advantage of the ACY1215-mediated enrichment of DN3b^{Pre} cells, and to compare effects of the drug on each stage (**Figure 6i**). After one day, only DN3b^{Post} cells had achieved the DP phenotype in substantial numbers, and this was reduced by ACY1215 in all three cases (Figure 6Aii). More informatively, CD28 and CD2 co-staining (Figure 6Aiii) indicated that after 1 day the majority of DN3a cells had progressed to DN3b^{Pre}, most DN3b^{Pre} cells were still DN3b^{Pre}, and most DN3b^{Post} cells were still DN3b^{Post} (Over 20% of the DN3b^{Pre} cells showed the DN3a phenotype after 1 day of culture, but this was most likely due to the low numbers of DN3b^{Pre} under DMSO treatment, and the difficulty of obtaining a clean discrimination between CD28^{Lo}and CD28^{Hi}cells). Culturing cells that had been pre-treated with ACY1215 before sorting showed a similar pattern of progression (although with fewer DN3a cells arising from the DN3b^{Pre} sort, consistent with these cells being more prominent and therefore less contaminated by DN3a cells during sorted). These data indicate that DN3b^{Pre} (CD28^{Lo}CD2^{Lo}) is a transitional state between DN3a (CD28^{Hi}CD2^{Lo}) and DN3b^{Post} (CD28^{Hi}CD2^{Hi}). Together with the previous observation that ACY1215 increases the proportion of this transitional stage by suppressing numbers of DN3a and DN3b^{Post}, these findings suggest that inhibition of HDCA6 both promotes progression from DN3a to DN3b^{Pre}, and prevents progression from DN3b^{Pre} to DN3b^{Post}.

ACY1215 alters the pre-TCR signalling platform clustered at MTOC

We explored three possible mechanisms by which ACY1215 might disrupts β-selection. ACY1215 is selective for HDAC6, and can inhibit the catalytic activity of HDAC6 (Eich et al., 2018; Narita et al., 2019). HDAC6 protein is expressed at every stage of T cell development (**Supp Fig 5**). The best known role of HDAC6 is in modification of histones for epigenetic regulation. Indeed, acetylation of

H3K18 was increased upon treatment with ACY1215, suggesting that epigenetic modification could be affected by the drug (Supp Fig 5).

Although best known as a regulator of histone acetylation, HDAC6 can also acetylate α-tubulin (Narita et al., 2019). In mature T cells, acetylation of α-tubulin by HDAC6 influences TCR-mediated recruitment of the microtubule-organising centre (MTOC) to the immunological synapse (Serrador et al., 2004). In both DN3a and DN3b cells, HDAC6 was predominantly in the nucleus, but detectable expression in the cytoplasm and near the MTOC was compatible with effects on MTOC modification (**Supp Fig 5**). We assessed the acetylation of α-tubulin (K40), which can be de-acetylated by HDAC6, on the sorted T cell populations: DN, DP, CD4-SP, CD8-SP, DN1, DN2, DN3a, and DN3b (**Figure 7A**). Upon a two-hour treatment with ACY1215, each population showed an increase in acetylated tubulin, suggesting HDAC6 is catalytically active throughout early T cell development.

We have previously found that T cells undergoing β-selection form an immunological synapse, in which MTOC and other TCR-associated signalling proteins move with the MTOC to the site of antigen receptor signalling receptor signalling (Allam et al., 2021). We therefore speculated that an alteration in MTOC organisation has the potential to mediate the effects of ACY1215 on β-selection by impacting the immunological synapse. To begin to address this, we looked at the association of LAT with the MTOC in DN3a cells (**Figure 7B**). Acetyl-α-tubulin presented as a single cluster in the site of the MTOC, and was increased in intensity with ACY1215 treatment, compatible with the flow cytometry results. LAT was strongly associated with the MTOC in DMSO treated cells, but altered by ACY1215 treatment, with less intense fluorescence and less clustering at the MTOC. Notch is particularly important during β-selection in mediating assembly of the immunological synapse and transmitting signals downstream of the pre-TCR signal (Allam et al., 2021; Charnley et al., 2020). We therefore assessed the co-localisation of Notch1 and the MTOC in DN3a cells (**Figure 7C**). In DMSO treated cells, Notch was concentrated at the MTOC, but, similar to LAT was much more diffuse following ACY1215 treatment. Interestingly, the change in localisation of Notch was accompanied by a loss in Notch1 expression, and this occurred in DN3a, DN3b and DN4 cells. These data suggest that ACY1215 treatment might accelerate the down-regulation of Notch1 that is a critical component of β-

selection (**Figure 7D**). These data suggest that one possible mechanistic basis for the effects of ACY1215 on β-selection is via tubulin acetylation and recruitment by MTOC of Notch1 and TCR signalling to the immunological synapse.

DN3b^{Pre} cells have commenced but not completed β-selection, and are controlled by sequential changes in key regulators of β-selection.

Two critical regulators of T cell development are the transcription factors TCF-1 and Lef1. Lef1 plays various roles throughout T cell development (Staal and Clevers, 2005). Lef1 was upregulated in a proportion of DMSO-treated DN3b cells, but this upregulation was not observed in ACY1215-treated cells (**Figure 8A**). TCF-1 and Lef1 can directly modify histone acetylation, and this function is inhibited by pharmacological HDAC inhibitors, Tubacin and Vorinostat, (Xing et al., 2016; Zhao et al., 2021). Parallels between the phenotype we observed and those observed with disruption of the transcription factors Lef1 and TCF-1 therefore suggested the possibility that ACY1215 might exert its effects via TCF-1 or Lef1 as well as, or instead of, HDAC6. Thus, both HDAC6 and Lef-1 are candidates to mediate the effect of ACY1215 on T cell development.

To assess a possible role for Lef1, we explored further how its expression changed with progression through β-selection, and how it was impacted by ACY1215 treatment. Co-staining DN3 cells with CD2 and Lef-1 (**Figure 8B)** indicated that their expression was tightly correlated, with all DN3a cells low for both proteins, and all DN3b^{Post} cells high for both proteins. DN3b^{Pre} cells showed around 35% fraction of CD2^{Lo}cells expressing Lef1, suggesting that CD2 is upregulated later than Lef1. The upregulation of Lef-1 in a subset of DN3b^{Pre} reduced to only 15% in the presence of ACY1215, reflecting the reduced Lef1 upregulation observed in total DN3b cells (Fig 8A). Strikingly, the ACY1215-treated DN3b^{Post} cells showed clear upregulation of Lef1 equivalent to that seen in the DMSO-treated cells. These data are compatible with a model in which DN3a cells upregulate CD28 to become DN3b^{Pre} cells, then upregulate Lef1, and finally upregulate CD2 to become DN3b^{Post} cells. Treatment with ACY1215 disrupts the Lef1 upregulation in the DN3b^{Pre} cells, without affecting Lef1 in the DN3b^{Post} stage.

Co-staining the different β-selection stages with Lef1 and icTCRβ indicated some degree of co-regulation of the two markers, with increasing Lef1 corresponding to an overall shift towards more positivity in icTCRβ. Interestingly, the small fraction of Lef1^{Hi}DN3b^{Pre} cells exhibited intermediate levels of icTCRβ compared with the Lef^{Lo}DN3b^{Pre} cells, which were negative for icTCRβ. This is compatible with two non-exclusive scenarios: these Lef1^{Hi}icTCRβ^{mid}CD2^{Lo}cells could be partway through β-selection, and about to transition to the DN3b^{post} stage, or they could be cells with flawed icTCRβ, unable to trigger the upregulation of CD2 and perhaps destined to die. In either case, the effect of ACY1215 is to prevent the upregulation of both Lef1 and icTCRβ at the DN3b^{Pre} stage, while allowing progression to the DN3b^{Post} stage.

Does the differential upregulation of Lef1 provide a clue as to ACY1215 targets during β-selection? Lef1 is actively suppressed by several mediators of T cell development, but it is not known what changes mediate its expression during β-selection. During T cell development, Lef1 expression is functionally redundant with, and inhibited by TCF-1 (Okamura et al., 1998; Yu et al., 2012), but TCF-1 is still active during β-selection (Okamura et al., 1998), suggesting it is not a candidate for the Lef1 upregulation we see in DN3b^{Pre} cells. Lef1 can be downregulated by active STAT5 (Gupta et al., 2014), suggesting a possible means for the expression profiles seen here. A key feature of progression through β-selection is changes in responsiveness to IL-7 signalling, with survival before β-selection dependent upon IL-7-induced Bcl-2 (Boudil et al., 2015). IL-7 inhibits expression of Lef1 and other regulators required for T cell development (Yu et al., 2004) so we assessed IL-7R expression and phosphorylation of its key mediator, STAT5 (**Supp Fig 6**). As previously found (Teague et al., 2010; Yu et al., 2004), both IL7R and phospho-Stat5 are reduced as cells pass through β-selection, IL7R expression *per se* is not altered by ACY1215 treatment, but phospho-STAT5 is down-regulated more rapidly by ACY treatment, suggesting that the drug might escalate the switching off of IL7R signalling. Expression of IL7R is negatively correlated with expression of Lef-1 in DN3b cells, compatible with an inhibition of Lef1 expression by IL7 signalling. STAT5 transcriptional activity has previously been found to be regulated by direct effects of HDAC6 on HMGN2 in breast cancer

cells (Medler et al., 2016). These data are compatible with the notion that, as cells enter the DN3b^{Pre} stage of β-selection, a downregulation of IL7 signalling might trigger expression of Lef-1

These findings all point to the hypothesis that the DN3b^{Pre} population is finely poised between failure of β-selection or progression through the β-selection checkpoint, and that ACY1215 disrupts this fine balance, leading to progression of cells without TCRβ. To explore this hypothesis further, we focussed on, CD5, which we had found to be uncoupled from expression of icTCRβ but still associated with proliferation (Figure 4). Co-staining CD5 and Lef1 (**Figure 9A**) indicated that cells progressively expressed both Lef1 and CD5 as they passed through β-selection, with the upregulation of Lef1 in DN3b^{Pre} cells tightly correlated with CD5 upregulation. Given the known role of CD5 as an indicator of TCR signalling, this reinforces the notion that, once DN3b^{Pre} cells have entered the β-selection checkpoint, they respond to effective pre-TCR signalling by expressing Lef1 and CD5. Passing of the β-selection checkpoint is then marked by the expression of CD2. Treatment with ACY1215 did not alter the upregulation of Lef-1, but prevented the upregulation of CD5. This lack of expression of CD5 provides one possible mechanism for the escape of cells lacking an appropriately rearranged TCRβ chain following ACY1215 treatment, although such a role remains to be investigated. Irrespective of any functional role for CD5, these data show both that CD5 reports pre-TCR signalling as has previously been shown for TCRαβ signalling (Azzam et al., 1998) (Sood et al., 2021; Tarakhovsky et al., 1995), and that this reporting is disrupted by ACY1215.

These data suggest a role for the coordinated expression of CD5 and Lef1 in the completion of the β-selection checkpoint. To confirm this, we made use of a previous observation (Ananias et al., 2008; Teague et al., 2010). A population with intermediate levels of CD25 has previously been identified within the DN3b population, and termed DN3c to indicate that it was a transitional stage between DN3b and DN4. We therefore assessed the relationship between CD2 and CD25 in the DN3b cells. The CD28^{Hi}CD2^{Lo}population encompassed some CD25^{int} cells, although many were still high for CD25 (**Supp Fig 7**). These data are compatible with the notion that DN3b^{post} marks a later stage in differentiation, that includes, but is not exclusive to, the DN3c population (Ananias et al., 2008). To assess whether the combined expression of CD5 and Lef1 in DN3b cells indicated progression

through β-selection, we gated for the two clearly discriminated sub-populations Lef1^{Lo}CD5^{Lo} and Lef1^{Hi}CD5^{Hi}, and compared their CD25 expression **(Figure 9B**). The Lef1^{Hi}CD5^{Hi} cells were substantially lower for CD25, indicating that they had already progressed through β-selection. Although as expected there were far fewer cells in the Lef1^{Hi}CD5^{Hi} population upon ACY1215 treatment, they also exhibited the reduction in CD25, indicating that the impact of the drug is upstream of CD5 expression. Together, these findings indicate that, following CD2 upregulation, cells report their nascent pre-TCR signalling via co-expression of CD5 and Lef1, with subsequent downregulation of CD25 marking completion of β-selection in the Lef1^{Hi}CD5^{Hi} cells.

Discussion

A critical factor in β-selection is the sequential expression of specific transcriptional regulators, with differential perdurance and cross-inhibition ensuring checks and balances that prevent inappropriate survival and differentiation (Chann and Russell, 2019; Zhao et al., 2021). Many such checks and balances have been identified to play important roles during β-selection, but the stepwise progression of events that dictate fate have been elusive (Chann and Russell, 2019; Zhao et al., 2021). In a new working model suggested by these results (**Figure 10, Supp Fig 8**), key steps in β-selection would involve the transmission of information from the nascent pre-TCR to CD5 and Lef, with CD5 dampening the pre-TCR signal. Cells that pass β-selection and complete recombination of the TCRβ gene activate expression of CD2 (marking transition from DN3b^{Pre} to DN3b^{Post}). Disruption of this sequence of events by ACY1215 impedes the differentiation from DN3b^{Pre} to DN3b^{Post}, prevents effective correlation of TCRβ signals with cell growth and proliferation, and subsequently leads to defective DN3b^{Post} cells that are unable to progress further in T cell development.

Here, our exploration of the effects of ACY1215 have pinpointed a pivotal stage in β-selection that is clearly book-ended by upregulation of TCR co-receptors: CD27 and CD28 at the start of DN3b^{Pre}, and CD2 at the transition to DN3b^{Post}. The upregulation of CD27 and CD28 is gradual, but the upregulation if CD2 is more abrupt, making for a convenient demarcation of differentiations stages. Our findings are compatible with previous observations that CD2 expression marks cells with TCRβ gene rearrangement (Rodewald et al., 1993), that knockout of CD2 inhibits progression to the DN4

stage but does not influence TCRβ repertoire (Sasada and Reinherz, 2001), and suggestions of cis-regulation of CD2 and TCRβ expression involving chromatin structure (Kamoun et al., 1995) Together, these findings suggest that expression of CD2 (marking entrance to the DN3b^{Post} stage) reflects a completion of TCRβ recombination and triggers critical fate-determining events that involve progressive upregulation of CD5 and Lef1. CD2 in mature T cells sets quantitative thresholds for activation (Bachmann et al., 1999), suggesting the possibility that a similar process could be involved in β-selection.

A second major finding from this work is that CD5 levels are modified according to pre-TCR expression, and that treatment with ACY1215 prevents the upregulation of CD5 (but does not disrupt Lef1 upregulation) during β-selection. At other stages of T cell development and activation, CD5 reports on the strength of TCR signalling, with increasing expression reflecting a stronger TCR signal (Azzam et al., 1998; Sood et al., 2021; Tarakhovsky et al., 1995). Our findings now suggest CD5 plays a similar role as a reporter of pre-TCR signalling. CD5 then negatively regulates TCR signalling, and the combined action of responding to, and dampening, the TCR signal, allows CD5 to tune the TCR signal and so shift the window and modify the timing of positive selection (Lutes et al., 2021; Matson et al., 2020; Sood et al., 2021; Voisinne et al., 2018). Interestingly, it is now emerging that differential CD5 expression also marks the propensity for different fates in thymocytes and CD4^{+} T cells, and this reflects transcriptional and epigenetic differences between cells with high and low CD5 expression (Rogers et al., 2021). A role for tuning of the TCRβ repertoire during β selection is made relevant by findings that the pre-TCR can bind with low affinity to MHC-peptide (Li et al., 2021; Mallis et al., 2015). The pre-TCR also forms an immunological synapse with many similarities to the immunological synapse formed by the αβTCR, oriented towards MHC (Allam et al., 2021). These recent observations support the notion that CD5 could play a similar role in both reporting and handicapping TCR signals. More work is needed to determine any functional connection between CD5 and epigenetic modifications during β-selection, but these data point to a role for CD5 during the DN3b^{Pre} stage in reporting, and perhaps tuning, pre-TCR activity to determine subsequent passage through the β-selection checkpoint.

The impact of ACY1215 on cellular phenotype and fate is clear, but the molecular basis for these effects needs more exploration. There are many possible means by which ACY1215 might impact upon transcriptional and epigenetic alterations during β-selection to mediate the phonotypes we observe here. It was recently shown that the transcriptional repressor, Bcl6, is required for passage through the β-selection checkpoint (Solanki et al., 2020). Several HDACs have been shown to complex with and modulate Bcl6 activity to impact on B cell development and function (Wang et al., 2020), suggesting the possibility that ACY1215 might mediate at least some of its effects via Bcl6. HDAC6 has also been implicated in the DNA damage response (Zhang et al., 2019), raising the possibility that ACY1215 effects might relate to the genetic recombination integral to the creation of a TCRβ chain (Miyazaki et al., 2008). It is well established that Notch induces expression of TCF-1 to drive T lineage specification and prevent T lymphoma development (Tiemessen et al., 2012; Weber et al., 2011). At β-selection, transient activation of β-catenin mediates TCF-1 and Lef1 transcriptional regulation to promote pre-TCR-dependent transition to the DN4 stage (Gounari et al., 2001). Ectopic expression of a constitutively active β-catenin allows the cells to bypass pre-TCR signalling, yielding DN4 cells lacking expression of TCRβ (Gounari et al., 2001). The similarities between this phenotype and the apparent bypass of pre-TCR signalling we observe with ACY1215 treatment suggested the possibility that TCF-1/Lef might be mediate the effects of ACY1215. Indeed, Lef1 was not induced in ACY1215-treated DN3b^{Pre} cells, despite being normally upregulated in ACY1215-treated DN3b^{Post} cells. These data suggest that Lef1 plays a stage-specific (DN3b^{Pre} stage) role in sensing the strength of pre-TCR signalling, and that this activity can be altered by ACY1215 treatment. Whether the effect of ACY1215 relates to HDAC6, an alternative HDAC, or the histone deacetylase activity of Lef1/TCF-1 remains to be determined. In any case, the functional outcome of ACY1215 treatment is to disrupt the connections between pre-TCR signalling strength and the expression of CD5 and Lef1. One explanation for this finding could be that HDAC6 normally retards upregulation of CD2 early in the β-selection process, allowing for an appropriate balance between the positive and negative effects of CD2 and CD5 on pre-TCR signalling. In this scenario, once a cell has progressed through β-selection (and so expresses CD5 and Lef1), high CD2 would be required to promote pre-TCR signalling and drive the cell through the DN4 and DP stage. Premature upregulation of CD2 by

ACY1215 treatment might then enable cells that had created a non-ideal TCRβ to survival inappropriately at the DN3b^{Pre} stage, but fail to progress to DN4.

To our knowledge, a functional relationship between Lef1 and CD5 has not previously been explored. However, our findings suggest a correlation in expression of the two proteins, most notably at at the DN3b^{Pre} stage when they are both increasing (Figure 9A). The pattern of expression of these markers supports the notion that Lef1 and CD5 link TCRβ expression to proliferation (Figure 4B) and to the completion of β-selection and transition to the DN4 stage (Figure 9B). Uncoupling CD5 from TCRβ and Lef1 expression provides a possible mechanism by which ACY1215 allows the wrong cells (perhaps cells without suitable TCRβ) to proliferate and differentiate to DN3b^{Post} cells, but these cells subsequently fail to progress, leading to the block in DP differentiation.

The known role for HDAC6 in linking tubulin acetylation to the immunological synapse of mature T cells (Serrador et al., 2004), and our finding that acetylation of α-tubulin is increased in DN3 cells, suggested the possibility that the β-selection immunological synapse might mediate the effects of ACY125. Indeed, ACY1215 does alter the organisation of the TCR signalling molecules, LAT, around the MTOC. Similarly, Notch1, which is required to enhance the polarisation of the pre-TCR (Allam et al., 2021; Charnley et al., 2020), is lost from the MTOC following ACY1215 treatment. These findings are particularly interesting in light of a recent report that HDAC6 is required for the formation of aggresomes at the MTOC (Magupalli et al., 2020), and suggest that HDAC6 might play a more general role in coordinating recruitment to the MTOC. An alternative explanation for the effect of ACY1215 on β-selection relates to observations that HDAC inhibitors can induce MHC constituents to promote antigen presentation (Magner et al., 2000). It remains to be determined whether an influence on stromal-presented peptide-MHC plays any role in disrupting β-selection. Interestingly, both CD2 and CD5 can regulate activity of the immunological synapse and connectivity to the MTOC (Brossard et al., 2003; Dustin et al., 1998; Tibaldi et al., 2002) further supporting the possibility that the immunological synapse provides a hub at which deacetylation and pre-TCR signalling converge. Together, these findings suggest that the effect of HDAC6 on β-selection that we see here might occur through disruption of the DN3 immunological synapse.

The molecular basis for the effects of ACY1215 on β-selection might therefore by multifaceted, and relate to one or more of direct alteration of the epigenome to influence protein expression, alteration of Lef1 activity, DNA damage response, alteration of pre-TCR signalling via organisation at the MTOC and the immunological synapse. Irrespective of the molecular mechanism, the finding that AY1215 disrupts T cell development has potential implications for the development of clinical applications of small molecule inhibitors of HDAC6, particularly in treatment of young patients, whose T cell repertoire has not yet been established (Cosenza and Pozzi, 2018; Hogg et al., 2020).

ACY1215 treatment has exposed the DN3b^{Pre} stage of β-selection, enabling us to identify a critical sequence of events that dictate cell fate during β-selection. We now propose a refined model of β-selection, in which the checkpoint marked by upregulation of CD28 involves a coordinated increase in expression of the pre-TCR and CD5, with an escalating requirement for pre-TCR signalling strength that, if met, culminates in the expression of CD2 and exit from the β-selection checkpoint.

Materials and Methods

Ex vivo generation of mouse primary thymocyte and drug treatments

Hematopoietic stem cells (HSC) were collected from C57BL/6 mouse E14.5 fetal liver. To induce T cell development, HSC were co-cultured with OP9-DL1 stromal cells (from Juan Carlos Zúñiga-Pflücker, University of Toronto, Toronto, Canada) at a 1:1 ratio in a 6-well plate (2×10^5). The coculture was maintained in αMEM (Sigma-Aldrich, M4526), supplemented with foetal calf serum (10% v/v), glutamine (1 mM), β-mercaptoethanol (50 μM), sodium pyruvate (1nM), HEPES (10 mM), penicillin/streptomycin (100 ng/mL), mouse interleukin 7 (1 ng/mL) and mouse

FMS-like tyrosine kinase 3 (5 ng/ml). For both Protocol 1 and Protocol 2 (Supp Fig 1), ACY1215 was purchased from MedChemExpress (NJ, USA) and used at 1 μM as described (Laino et al., 2019). ACY1215 was dissolved in DMSO to 5 mM, and diluted to 1 μM with culture media immediately prior to application to cells. The small-molecule inhibitor of Stat5, Pimozide (CAS 2062-78-4 Sigma-Aldrich) was used at a final concentration of 10 μM. The selective inhibitor of p300 and CBP, C646

(Sigma-Aldrich) was used at 2.5 μM. OP9-DL1 stromal cells was maintained in αMEM (Sigma-Aldrich, M4526) supplemented with 20% (v/v) fetal calf serum, glutamine (1 mM) and penicillin/streptomycin (100 ng/mL). When OP9-DL1 stromal cells were confluent after 3-4 days of coculture, primary thymocytes were dissociated from the stromal cells through forceful pipetting, and were harvested with the fresh OP9-DL1 stromal cells.

Flow Cytometry and FACS

To purify T cell populations using flow cytometry, primary thymocytes were dissociated from OP9-DL1 stromal cell, and were resuspended in PBS buffer containing 2% FBS and antibody cocktail for surface staining. Antibody cocktails were comprised of lineage markers (NK-1.1, CD11b, CD45R, Ly6G6C, Ter119), and differentiation markers (CD4, CD8, CD25, CD44, CD28 and CD2; details about fluorochrome, manufacturer and dilution are summarised in the supplementary materials). Primary thymocytes were incubated with antibody cocktails for 40 minutes before FACS.

Flow cytometry (BD Aria III) was used to analyse and sort the populations of developing T cells. DN3 cells were identified based on surface expression (Lineage^{-}, CD4^{-}, CD8^{-}, CD25^{Hi}, CD44^{Lo}). DN3a cells were DN3 cell with CD28^{L0}, by contrast, DN3b cells were DN3 cell with CD28^{Hi}. DP cells were identified based on surface expression (Lineage^{-}, CD4^{+}, CD8^{+}).

Intracellular staining for flow cytometry

To detect intracellular expression of TCRβ, Ki67, Lef1, c-Myc, Notch1, HDAC6 and H3K18ac, the Foxp3/Transcription Factor Staining Buffer Kit (eBioscience) was used according to the manufacturer's instruction. Briefly, the primary thymocytes after surface staining were incubated with fixative for 15 minutes in dark, room temperature, followed with centrifuge and washing out the fixative. To detect expression of acetyl-tubulin, the cells were fixed with IC Fixation Buffer (eBioscience) for 15 minutes in dark, room temperature, followed with centrifuge and washing out the fixative. The fixed cells were then incubated with antibody for flow cytometry analysis.

Immunofluorescence staining and confocal microscopy

The sorted DN3a or DN3b were grown on glass-bottomed 8-well chambers (ibidi) with OP9-DL1 stromal cells, and were fixed with 4% formaldehyde for 8 minutes at room temperature followed by 0.1% Triton X-100 permeabilization for 5 minutes. The samples were then incubated with primary antibody overnight at 4°C (details about antibody usage is summarised in Supplementary table 1). After the primary antibody being washed out by PBS, the cells were labelled with fluorochrome-conjugated secondary antibodies (as Table S1), DAPI (Thermo Fisher Scientific), and Phalloidin (Abcam). The samples were examined using a FV3000 confocal microscope (Olympus) and 60X lens (1.30 NA, UPLSAPO, Olympus). The images were processed with maximum intensity projection using Image J. The mean intensity of region of interest was examined in Image J.

Data collection and Statistical analyses

MATLAB (version R2021a) and Python (version 3.8.1) were used to visualise the statistics. Data of flow cytometry were analysed by FlowJo software (version X10.0.7r2. Tree Star, Inc.). The bar plot was shown as mean ± SEM. More than three repeats were included in the statistics and were colour-coded for each individual repeat. Microsoft Excel (version 2016) was used for t-test.

Acknowledgements

This work was done on Wurundjeri land of the Kulin nation, and we pay our respects to the Elders past and present. We thank Louise Cheng, Callum Dark, Amr Allam for technical assistance and helpful discussions, and Ellis Reinherz, Jonathon Duke-Cohan for helpful comments on the manuscript. The work was funded by Australian Research Council (FT0990405 to SMR), National Health and Medical Research Council (APP1099140 to SMR), Swinburne University Postgraduate Research Award to ASC.

Conflict of Interest Statement

No author declares a conflict of interest

Author Contribution Statement

Conceptualization: ASC, SMR
Methodology: ASC, MC, SMR
Experimentation: ASC
Visualization: ASC, SMR
Supervision: POH, RWJ, SMR
Writing—original draft: ASC, SMR
Writing—review & editing: ASC, MC, LN, AN, POH, RWJ, SMR

Ethics

C57bl/6 mouse E14.5 fetal livers were collected according to La Trobe University Animal Ethics Committee approval AEC-20024 and Peter MacCallum Cancer Centre Ethics Committee approval E627.

Figure Legends

Figure 1. ACY1215 arrests T cell development at DN3 stage

(A) A schematic of the stages of T cell development and the cell surface markers used to differentiate them. Cells were classed as DN (Double Negative, lacking expression of CD4 and CD8), and

progressed from DN1 to DN4 according to their expression of CD44 and CD25 as indicated (the quadrants are arranged as in Figure 1Aii below). β-selection occurs at the DN3 stage, as cells progress from DN3a to DN3b, indicated by upregulation of CD28. Cells progressed from DN4 to the DP stage (Double Positive, expressing both CD4 and CD8) before committing to SP (Single Positive for either CD4 or CD8, quadrants as in Figure 1Ai below). Developing T cells were treated with ACY1215 or DMSO for 2 days as indicated, and the Lin^- cells were assessed for CD4 and CD8 expression to determine the proportions of DN, DP, $CD8^+$ and $CD4^+$ populations **(i)**. The DN (Lin^-, $CD4^-$, $CD8^-$) cells from (i) were assessed for CD44 and CD25 expression to determine the proportions of DN3 and DN4 populations **(ii)**. The frequency of each population was summarised in a swarm plot, with individual colours representing each experiment. **(B)** The sorted DN3b cells were cultured for 4 days under ACY1215 or DMSO treatment as indicated, and were analysed by CD4 and CD8 **(i)** and CD44 and CD25 **(ii)**. The frequency of each population were summarised in swarm plot, with individual colours representing each experiment. Cell numbers per population were estimated by multiplying the total cell number by the frequency and were summarised in the line chart **(iii)**.

Figure 2. ACY1215 impairs the development of TCRβ lineage

(A) Developing T cells were treated with ACY1215 or DMSO for 2 days as indicated, and DN3a, DN3b, DN4 and DP cells were assessed for surface TCRβ and TCRγδ expression. **(B)** The sorted DN3b cells were cultured for 2 days under ACY1215 or DMSO treatment as indicated, and DN3, DN4 and DP cells were assessed for surface TCRβ and TCRγδ expression. **(C)** The sorted DN3b cells were cultured for 4 days under ACY1215 or DMSO treatment as indicated, and DN3, DN4 and DP cells were assessed for intracellular TCRβ (icTCRβ) and CD28 expression. The frequency and cell number were summarised in swarm plot, with individual colours representing each experiment.

Figure 3. ACY1215 impairs DN3a amplification

(A) The sorted DN3a cells were cultured under ACY1215 or DMSO treatment for 2 days as indicated, and the $CD44^-$ DN population (representing DN3 and DN4 stages) was assessed for CD25 and CD28 expression. The frequency of each population were summarised in swarm plots, with individual

colours representing each experiment. Cell numbers were summarised in line plots. **(B)** Developing T cells were treated with ACY1215 or DMSO for 1 day or 2 days, and the DN3 cells were assessed for CD27 and CD28 expression to discriminate DN3a and DN3b. Cell number were summarised in the swarm plot, with individual colours representing each experiment. **(C)** The sorted DN3a, DN3b and DP cells were treated with ACY1215 or DMSO for 3 hours or 6 hours as indicated, followed with propidium iodide (PI) staining to label dead cells. The frequency of PI^+ population were summarised in swarm plot, with individual colours representing each experiment. **(D)** The sorted DN3a and DN3b were stained with CFSE after sorting and were cultured with ACY1215 or DMSO for two days as indicated. At one hour post sorting, the intensity of CFSE were recorded, as indicated by the white histogram. At two days, the DN3 cells from the sorted DN3a and DN3b were assessed for CD28 expression and CFSE intensity, as shown in the contour plots and the histograms. **(E)** Developing T cells were treated with ACY1215 or DMSO for 1 day as indicated, and DN3a and DN3b cells were assessed for FSC and Ki-67 expression.

Figure 4. DN3b cells under ACY1215 treatment unlikely form normal pre-TCR signalling

(A) The sorted DN3a cells were cultured under ACY1215 or DMSO treatment for 4 days as indicated, and DN3 cells were assessed for the expressions of intracellular TCRβ (icTCRβ) versus CD28 or CD27. The frequency of $icTCR\beta^+$ cells was summarised in a swarm plot, with individual colours representing each experiment. **(B)** Developing T cells were treated with ACY1215 or DMSO for 2 day as indicated, and DN3 cells were assessed for CD5 and CD28 expression. CD5 MFI were summarised in the swarm plot, with individual colours representing each experiment. **(C)** The sorted DN3a and DN3b cells were treated with ACY1215 or DMSO for 2 days as indicated, and the DN3b cells were assessed for icTCRβ and CD5 expression. For $icTCR\beta^+$ DN3b cells, the proportions of $CD5^+$ or $CD5^-$ were summarised in the stacked column (n=3). **(D)** The sorted DN3a and DN3b were stained with CFSE after sorting and were cultured with ACY1215 or DMSO for two days as indicated. At two days, the DN3 cells from the sorted DN3a and DN3b were assessed for CD5 expression versus CFSE intensity.

Figure 5. CD2 upregulation discriminates DN3b^{Pre} and DN3b^{Post} populations

(A) Developing T cells were treated with ACY1215 or DMSO for 1 or 2 days, and the DN3 cells were assessed for CD2 and CD28 expression. As indicated in the schematic frequency and cell number of the three populations (DN3a, DN3b^{Pre}, and DN3b^{Post}) was summarised in swarm plots, with individual colours representing each experiment. **(B, D)** Developing T cells were treated with ACY1215 or DMSO for 1 day, and DN3a, DN3b^{Pre}, and DN3b^{Post} cells were assessed for icTCRβ, Ki-67 and c-Myc expression. MFI of icTCRβ, Ki-67 and c-Myc were summarised in histogram and swarm plot, with individual colours representing each experiment. **(C)** The sorted DN3a and DN3b were stained with CFSE after sorting and were cultured with ACY1215 or DMSO for two days as indicated. At two days, the DN3 cells from the sorted DN3a and DN3b were assessed for CD2 expression versus CFSE intensity.

Figure 6. Progression of DN3a, DN3b^{pre} and DN3b^{post} cells

(A) The developing T cells were treated with DMSO or ACY1215 for 1.5 day, and the DN3a, DN3b^{Pre}, and DN3b^{Post} cells were sorted as indicated **(i)**. At one day, the cells were analysed by CD4 and CD8 **(ii)** and CD2 and CD28 **(iii)**. The frequencies of each population were summarised in the line plots.

Figure 7. ACY1215 alters pre-TCR signalling clustered at MTOC.

(A) The sorted DN, DP, CD4-SP, CD8-SP, DN1, DN2, DN3a, DN3b were treated with ACY1215 or DMSO for 2 hours as indicated, and were assessed for acetyl-α-tubulin (K40) as shown in histograms.

(B, C) The sorted DN3a cells were treated with ACY1215 or DMSO for 1 day as indicated, followed by immunostaining for LAT, acetyl-α-tubulin (K40), Notch1 and α-tubulin. The mean intensity of acetyl-α-tubulin, LAT and the ratio of Notch1 expressed at MTOC versus at nucleus were summarized in violin plot overlaid with box plot. **(D)** Developing T cells were treated with ACY1215 or DMSO for 2 day, and the DN3a, DN3b and DN4 cells were assessed for Notch1 expression, as summarised in swarm plot, with individual colours representing each experiment.

Figure 8. Lef1 is upregulated from DN3b^{pre}

(A) Developing T cells were treated with ACY1215 or DMSO for 2 day as indicated, and DN3 cells were assessed for Lef1 and CD28 expression. **(B)** Developing T cells were treated with ACY1215 or DMSO for 1 day, and DN3a, DN3b^{Pre}, and DN3b^{Post} cells were assessed for Lef1 and icTCRβ expression **(i)**. The frequency of Lef1^{+} were summarised in swarm plot, with individual colours representing each experiment.

Figure 9. Correlation of CD5 and Lef1 in DN3a, DN3bPre, and DN3bPost cells

(A) Developing T cells were treated with ACY1215 or DMSO for 1 day as indicated, and DN3a, DN3b^{Pre}, and DN3b^{Post} cells were assessed for Lef1 and CD2 expression. DN3b^{Pre} cells were further characterised by Lef1^{Hi}or Lef1^{Lo}, and were assessed for Lef1 and CD5 expression with DN3a and DN3b^{Pre}. **(B)** Developing T cells were treated with ACY1215 or DMSO for 2 day as indicated, and DN3a and DN3b were assessed for Lef1 and CD5 expression. The expression of CD25 in the DN3b subsets were shown in histogram. MFI of CD5 (A) and MFI of CD25 (B) were summarised in swarm plot, with individual colours representing each experiment.

Figure 10. Proposed stepwise progression through distinct stages of β-selection.

(A) Schematic summarises the working model of molecular interactions during β-selection. Firstly, cells first upregulate CD28 (the defining step in transition from DN3a to DN3b^{Pre}) which acts to promote signalling through the nascent pre-TCR. Second, pre-TCR signals induce expression of CD5, which might subsequently dampen the pre-TCR signal, perhaps leading to more rigorous selective pressure. Third, cells that pass the checkpoint upregulate CD2 (the transition from DN3b^{Pre} to DN3b^{Post}), which facilitates survival, proliferation and further differentiation. The co-receptors CD28, CD5, and CD2 all have the potential to accumulate at immunological synapse to mediate pre-TCR engagement with MHC-peptide. Treatment with ACY1215 disrupts acetylation of tubulin and H3K18, and assembly of key immunological synapse components at the MTOC subsequently disrupting the

functional link between CD5 and cell proliferation, **(B)** Schematic shows the sequence of protein expression changes during development from DN3a, DN3b^{Pre} to DN3b^{Post}.

Figure S1.

(A) Two protocols used throughout this study. Briefly, in Protocol 1, the developing T cells were treated with ACY1215 or DMSO, followed by flow cytometry analysis. In Protocol 2, the sorted T cells were treated with ACY1215 or DMSO, and followed by flow cytometry analysis. For both Protocol 1 and 2, the gating strategy at the starting day is indicated in **(B)**.

Figure S2.

(A) The sorted DN3a were cultured for 4 days under ACY1215 or DMSO treatment as indicated, and were analysed by CD4 and CD8 **(i)** and CD44 and CD25 **(ii)**. The frequency of each population was summarised in swarm plot, with individual colours representing independent experiments. (B) The sorted DN2, DN3a, DN3b and DP were cultured for 2 days ACY1215 or DMSO treatment as indicated. Cell numbers were counted at 3 hours and 2 days, and the proliferation rate (2 days / 3 hours) was summarised in swarm plot, with individual colours representing independent experiments.

Figure S3.

CD28 upregulation marks both DN3 cells differentiation and passing β-selection. Developing T cells at around day 9 of coculture with OP9-DL1 stromal cells were assessed for CD28, CD71, CD98, CD27 and surface TCRβ expression.

Figure S4.

The sorted DN3a and DN3b cells were treated with ACY1215 or DMSO for 6 hours or 1 day with or without OP9-DL1 coculture as indicated. The cells were assessed for Annexin V expression and DAPI intensity as shown in the density plot.

Figure S5.

HDAC6 is expressed in developing T cells. **(A)** Developing T cells were treated with ACY1215, the selective inhibitor of p300 and CBP, C646, or DMSO for 1 day as indicated, and the expression of H3K18ac were assessed and shown in the histogram. **(B)** To examine HDAC6 protein expression, developing T cells treated with DMSO or ACY1215 for two days were fixed by cytoplasmic fixative or nuclear fixative, followed by examination of HDAC6 expression. **(C)** The sorted DN3a or DN3b cells were assessed for HDAC6 expression by immunostaining. **(D, E)** The sorted DN3b cells were treated with ACY1215 or DMSO for 1 day, followed by immunostaining for Arp2, acetyl-α-tubulin (K40), and α-tubulin.

Figure S6.

Developing T cells were treated with ACY1215, Pimozide (Stat5 inhibitor) or DMSO for 2 days, and IL7R expression of DN1, DN2, DN3a, DN3b and DN4 cells were shown in the histograms **(A)**, or phosphorylated Stat5 of DN3a, DN3b and DN4 cells were summarised the swarm plot, with individual colours representing independent experiments **(B)**. Developing T cells were treated with ACY1215 or DMSO for 2 day as indicated, and DN3b cells with Lef1^{Hi}and Lef1^{Lo} were assessed for IL7R expression.

Figure S7.

(B) Developing T cells were treated with ACY1215 or DMSO for 1.5 day, and the DN3 subpopulations with CD28^{L0}CD2^{LOW}, CD28^{Hi}CD2^{Lo} or CD28^{Hi}/CD2^{Hi} were sorted as indicated. At day1, the 6 sorted DN3 cells subpopulations were discriminated for CD28^{Lo}CD2^{Lo}, CD28^{Hi}CD2^{Lo} or CD28^{Hi}CD2H^{i} expression and were assessed with CD25 expression, as shown in the contour plots and histograms

Figure S8.

Schematic illustrates how expression of each surface marker impacts upon progression through β-selection via DN3a, DN3b^{Pre} to DN3b^{Post} stages.

Adeegbe, D.O., Y. Liu, P.H. Lizotte, Y. Kamihara, A.R. Aref, C. Almonte, R. Dries, Y. Li, S. Liu, X. Wang, T. Warner-Hatten, J. Castrillon, G.C. Yuan, N. Poudel-Neupane, H. Zhang, J.L. Guerriero, S. Han, M.M. Awad, D.A. Barbie, J. Ritz, S.S. Jones, P.S. Hammerman, J. Bradner, S.N. Quayle, and K.K. Wong. 2017. Synergistic Immunostimulatory Effects and Therapeutic Benefit of Combined Histone Deacetylase and Bromodomain Inhibition in Non-Small Cell Lung Cancer. *Cancer discovery* 7:852-867.

Allam, A.H., M. Charnley, K. Pham, and S.M. Russell. 2021. Developing T cells form an immunological synapse for passage through the beta-selection checkpoint. *J Cell Biol* 220:

Ananias, H.J., I.J. de Jong, R.A. Dierckx, C. van de Wiele, W. Helfrich, and P.H. Elsinga. 2008. Nuclear imaging of prostate cancer with gastrin-releasing-peptide-receptor targeted radiopharmaceuticals. *Current pharmaceutical design* 14:3033-3047.

Azzam, H.S., J.B. DeJarnette, K. Huang, R. Emmons, C.-S. Park, C.L. Sommers, D. El-Khoury, E.W. Shores, and P.E. Love. 2001. Fine Tuning of TCR Signaling by CD5. *The Journal of Immunology* 166:5464-5472.

Azzam, H.S., A. Grinberg, K. Lui, H. Shen, E.W. Shores, and P.E. Love. 1998. CD5 expression is developmentally regulated by T cell receptor (TCR) signals and TCR avidity. *J Exp Med* 188:2301-2311.

Bachmann, M.F., M. Barner, and M. Kopf. 1999. CD2 sets quantitative thresholds in T cell activation. *J Exp Med* 190:1383-1392.

Ballesteros-Arias, L., J.G. Silva, R.A. Paiva, B. Carbonetto, P. Faisca, and V.C. Martins. 2019. T Cell Acute Lymphoblastic Leukemia as a Consequence of Thymus Autonomy. *J Immunol*

Boudil, A., I.R. Matei, H.Y. Shih, G. Bogdanoski, J.S. Yuan, S.G. Chang, B. Montpellier, P.E. Kowalski, V. Voisin, S. Bashir, G.D. Bader, M.S. Krangel, and C.J. Guidos. 2015. IL-7 coordinates proliferation, differentiation and Tcra recombination during thymocyte beta-selection. *Nat Immunol* 16:397-405.

Brossard, C., M. Semichon, A. Trautmann, and G. Bismuth. 2003. CD5 inhibits signaling at the immunological synapse without impairing its formation. *J Immunol* 170:4623-4629.

Carr, T., V. Krishnamoorthy, S. Yu, H.-H. Xue, B.L. Kee, and M. Verykokakis. 2015. The transcription factor lymphoid enhancer factor 1 controls invariant natural killer T cell expansion and Th2-type effector differentiation. *Journal of Experimental Medicine* 212:793-807.

Chann, A.S., and S.M. Russell. 2019. An integrated transcriptional switch at the beta-selection checkpoint determines T cell survival, development and leukaemogenesis. *Biochemical Society transactions* 47:1077-1089.

Charnley, M., M. Ludford-Menting, K. Pham, and S.M. Russell. 2020. A new role for Notch in the control of polarity and asymmetric cell division of developing T cells. *J Cell Sci* 133:jcs235358.

Ciofani, M., and J.C. Zuniga-Pflucker. 2005. Notch promotes survival of pre-T cells at the beta-selection checkpoint by regulating cellular metabolism. *Nat Immunol* 6:881-888.

Cosenza, M., and S. Pozzi. 2018. The Therapeutic Strategy of HDAC6 Inhibitors in Lymphoproliferative Disease. *International journal of molecular sciences* 19:

Douek, D.C., R.A. Vescio, M.R. Betts, J.M. Brenchley, B.J. Hill, L. Zhang, J.R. Berenson, R.H. Collins, and R.A. Koup. 2000. Assessment of thymic output in adults after haematopoietic stem-cell transplantation and prediction of T-cell reconstitution. *Lancet* 355:1875-1881.

Dustin, M.L., M.W. Olszowy, A.D. Holdorf, J. Li, S. Bromley, N. Desai, P. Widder, F. Rosenberger, P.A. van der Merwe, P.M. Allen, and A.S. Shaw. 1998. A novel adaptor protein orchestrates receptor patterning and cytoskeletal polarity in T-cell contacts. *Cell* 94:667-677.

Dutta, A., B. Zhao, and P.E. Love. 2021. New insights into TCR β-selection. *Trends in Immunology*

Eich, C., J. Arlt, C.S. Vink, P. Solaimani Kartalaei, P. Kaimakis, S.A. Mariani, R. van der Linden, W.A. van Cappellen, and E. Dzierzak. 2018. In vivo single cell analysis reveals Gata2 dynamics in cells transitioning to hematopoietic fate. *The Journal of Experimental Medicine* 215:233-248.

Gerdes, J., H. Lemke, H. Baisch, H.H. Wacker, U. Schwab, and H. Stein. 1984. Cell cycle analysis of a cell proliferation-associated human nuclear antigen defined by the monoclonal antibody Ki-67. *J Immunol* 133:1710-1715.

Gounari, F., I. Aifantis, K. Khazaie, S. Hoeflinger, N. Harada, M.M. Taketo, and H. von Boehmer. 2001. Somatic activation of beta-catenin bypasses pre-TCR signaling and TCR selection in thymocyte development. *Nat Immunol* 2:863-869.

Groettrup, M., A. Baron, G. Griffiths, R. Palacios, and H. von Boehmer. 1992. T cell receptor (TCR) beta chain homodimers on the surface of immature but not mature alpha, gamma, delta chain deficient T cell lines. *EMBO J* 11:2735-2745.

Gupta, K., I. Kuznetsova, O. Klimenkova, M. Klimiankou, J. Meyer, M.A. Moore, C. Zeidler, K. Welte, and J. Skokowa. 2014. Bortezomib inhibits STAT5-dependent degradation of LEF-1, inducing granulocytic differentiation in congenital neutropenia CD34(+) cells. *Blood* 123:2550-2561.

Hao, Y.-H., M.C. Lafita-Navarro, L. Zacharias, N. Borenstein-Auerbach, M. Kim, S. Barnes, J. Kim, J. Shay, R.J. DeBerardinis, and M. Conacci-Sorrell. 2019. Induction of LEF1 by MYC activates the WNT pathway and maintains cell proliferation. *Cell Communication and Signaling* 17:129.

Hayday, A.C., and D.J. Pennington. 2007. Key factors in the organized chaos of early T cell development. *Nat Immunol* 8:137-144.

Hogg, S.J., P.A. Beavis, M.A. Dawson, and R.W. Johnstone. 2020. Targeting the epigenetic regulation of antitumour immunity. *Nature reviews. Drug discovery*

Kamoun, M., J.S. Woods, N. Sano, H. Makni, R. Smith, W.B. de Lau, A. van Oers, D. Wotton, M.J. Owen, Y. Hashimoto, and H.C. Clevers. 1995. Analysis of CD2 and TCR-beta gene expression in Jurkat cell mutants suggests a cis regulation of gene transcription. *J Immunol* 155:3929-3937.

Laino, A.S., B.C. Betts, A. Veerapathran, I. Dolgalev, A. Sarnaik, S.N. Quayle, S.S. Jones, J.S. Weber, and D.M. Woods. 2019. HDAC6 selective inhibition of melanoma patient T-cells augments anti-tumor characteristics. *Journal for immunotherapy of cancer* 7:33.

Li, X., R. Mizsei, K. Tan, R.J. Mallis, J.S. Duke-Cohan, A. Akitsu, P.W. Tetteh, A. Dubey, W. Hwang, G. Wagner, M.J. Lang, H. Arthanari, J.H. Wang, and E.L. Reinherz. 2021. Pre-T cell receptors topologically sample self-ligands during thymocyte beta-selection. *Science* 371:181-185.

Lutes, L.K., Z. Steier, L.L. McIntyre, S. Pandey, J. Kaminski, A.R. Hoover, S. Ariotti, A. Streets, N. Yosef, and E.A. Robey. 2021. T cell self-reactivity during thymic development dictates the timing of positive selection. *eLife* 10:e65435.

Magner, W.J., A.L. Kazim, C. Stewart, M.A. Romano, G. Catalano, C. Grande, N. Keiser, F. Santaniello, and T.B. Tomasi. 2000. Activation of MHC class I, II, and CD40 gene expression by histone deacetylase inhibitors. *J Immunol* 165:7017-7024.

Magupalli, V.G., R. Negro, Y. Tian, A.V. Hauenstein, G. Di Caprio, W. Skillern, Q. Deng, P. Orning, H.B. Alam, Z. Maliga, H. Sharif, J.J. Hu, C.L. Evavold, J.C. Kagan, F.I. Schmidt, K.A. Fitzgerald, T. Kirchhausen, Y. Li, and H. Wu. 2020. HDAC6 mediates an aggresome-like mechanism for NLRP3 and pyrin inflammasome activation. *Science* 369:eaas8995.

Mallis, R.J., K. Bai, H. Arthanari, R.E. Hussey, M. Handley, Z. Li, L. Chingozha, J.S. Duke-Cohan, H. Lu, J.H. Wang, C. Zhu, G. Wagner, and E.L. Reinherz. 2015. Pre-TCR ligand binding impacts thymocyte development before alphabetaTCR expression. *Proc Natl Acad Sci U S A* 112:8373-8378.

Matson, C.A., S. Choi, F. Livak, B. Zhao, A. Mitra, P.E. Love, and N.J. Singh. 2020. CD5 dynamically calibrates basal NF-kappaB signaling in T cells during thymic development and peripheral activation. *Proc Natl Acad Sci U S A* 117:14342-14353.

Medler, T.R., J.M. Craig, A.A. Fiorillo, Y.B. Feeney, J.C. Harrell, and C.V. Clevenger. 2016. HDAC6 Deacetylates HMGN2 to Regulate Stat5a Activity and Breast Cancer Growth. *Molecular cancer research : MCR* 14:994-1008.

Miller, I., M. Min, C. Yang, C. Tian, S. Gookin, D. Carter, and S.L. Spencer. 2018. Ki67 is a Graded Rather than a Binary Marker of Proliferation versus Quiescence. *Cell reports* 24:1105-1112.e1105.

Miyazaki, M., K. Miyazaki, M. Itoi, Y. Katoh, Y. Guo, R. Kanno, Y. Katoh-Fukui, H. Honda, T. Amagai, M. van Lohuizen, H. Kawamoto, and M. Kanno. 2008. Thymocyte proliferation induced by pre-T cell receptor signaling is maintained through polycomb gene product Bmi-1-mediated Cdkn2a repression. *Immunity* 28:231-245.

Narita, T., B.T. Weinert, and C. Choudhary. 2019. Functions and mechanisms of non-histone protein acetylation. *Nature Reviews Molecular Cell Biology* 20:156-174.

Notarangelo, L.D., R. Bacchetta, J.L. Casanova, and H.C. Su. 2020. Human inborn errors of immunity: An expanding universe. *Science Immunology* 5:eabb1662.

Okamura, R.M., M. Sigvardsson, J. Galceran, S. Verbeek, H. Clevers, and R. Grosschedl. 1998. Redundant regulation of T cell differentiation and TCRalpha gene expression by the transcription factors LEF-1 and TCF-1. *Immunity* 8:11-20.

Rodewald, H.R., K. Awad, P. Moingeon, L. D'Adamio, D. Rabinowitz, Y. Shinkai, F.W. Alt, and E.L. Reinherz. 1993. Fc gamma RII/III and CD2 expression mark distinct subpopulations of immature CD4-CD8- murine thymocytes: in vivo developmental kinetics and T cell receptor beta chain rearrangement status. *J Exp Med* 177:1079-1092.

Rogers, D., A. Sood, H. Wang, J.J.P. van Beek, T.J. Rademaker, P. Artusa, C. Schneider, C. Shen, D.C. Wong, M.-È. Lebel, S.A. Condotta, M.J. Richer, A.J. Martins, J.S. Tsang, L. Barreiro, P. Francois, D. Langlais, H.J. Melichar, J. Textor, and J.N. Mandl. 2021. Pre-existing chromatin accessibility and gene expression differences among naïve CD4⁺ T cells influence effector potential. *bioRxiv* 2021.2004.2021.440846.

Sasada, T., and E.L. Reinherz. 2001. A critical role for CD2 in both thymic selection events and mature T cell function. *J Immunol* 166:2394-2403.

Serrador, J.M., J.R. Cabrero, D. Sancho, M. Mittelbrunn, A. Urzainqui, and F. Sanchez-Madrid. 2004. HDAC6 deacetylase activity links the tubulin cytoskeleton with immune synapse organization. *Immunity* 20:417-428.

Shapiro, M.J., and V.S. Shapiro. 2020. Chromatin-Modifying Enzymes in T Cell Development. *Annu Rev Immunol* 38:397-419.

Skånland, Sigrid S., K. Moltu, T. Berge, Einar M. Aandahl, and K. Taskén. 2014. T-cell co-stimulation through the CD2 and CD28 co-receptors induces distinct signalling responses. *Biochemical Journal* 460:399-410.

Solanki, A., D.C. Yánez, C.-I. Lau, J. Rowell, A. Barbarulo, S. Ross, H. Sahni, and T. Crompton. 2020. The transcriptional repressor Bcl6 promotes pre-TCR-induced thymocyte differentiation and attenuates Notch1 activation. *Development* 147:dev192203.

Sood, A., M.E. Lebel, M. Dong, M. Fournier, S.J. Vobecky, E. Haddad, J.S. Delisle, J.N. Mandl, N. Vrisekoop, and H.J. Melichar. 2021. CD5 levels define functionally heterogeneous populations of naive human CD4(+) T cells. *Eur J Immunol* 51:1365-1376.

Staal, F.J., and H.C. Clevers. 2005. WNT signalling and haematopoiesis: a WNT-WNT situation. *Nat Rev Immunol* 5:21-30.

Taghon, T., M.A. Yui, R. Pant, R.A. Diamond, and E.V. Rothenberg. 2006. Developmental and molecular characterization of emerging beta- and gammadelta-selected pre-T cells in the adult mouse thymus. *Immunity* 24:53-64.

Tarakhovsky, A., S.B. Kanner, J. Hombach, J.A. Ledbetter, W. Muller, N. Killeen, and K. Rajewsky. 1995. A role for CD5 in TCR-mediated signal transduction and thymocyte selection. *Science* 269:535-537.

Teague, T.K., C. Tan, J.H. Marino, B.K. Davis, A.A. Taylor, R.W. Huey, and C.J. Van De Wiele. 2010. CD28 expression redefines thymocyte development during the pre-T to DP transition. *Int Immunol* 22:387-397.

Tibaldi, E.V., R. Salgia, and E.L. Reinherz. 2002. CD2 molecules redistribute to the uropod during T cell scanning: implications for cellular activation and immune surveillance. *Proc Natl Acad Sci U S A* 99:7582-7587.

Tiemessen, M.M., M.R. Baert, T. Schonewille, M.H. Brugman, F. Famili, D.C. Salvatori, J.P. Meijerink, U. Ozbek, H. Clevers, J.J. van Dongen, and F.J. Staal. 2012. The nuclear effector of Wnt-signaling, Tcf1, functions as a T-cell-specific tumor suppressor for development of lymphomas. *PLoS Biol* 10:e1001430.

Tsuji, G., N. Okiyama, V.A. Villarroel, and S.I. Katz. 2015. Histone deacetylase 6 inhibition impairs effector CD8 T-cell functions during skin inflammation. *J Allergy Clin Immunol* 135:1228-1239.

Voisinne, G., A. Gonzalez de Peredo, and R. Roncagalli. 2018. CD5, an Undercover Regulator of TCR Signaling. *Frontiers in immunology* 9:

Wang, P., Z. Wang, and J. Liu. 2020. Role of HDACs in normal and malignant hematopoiesis. *Molecular cancer* 19:5.

Weber, B.N., A.W. Chi, A. Chavez, Y. Yashiro-Ohtani, Q. Yang, O. Shestova, and A. Bhandoola. 2011. A critical role for TCF-1 in T-lineage specification and differentiation. *Nature* 476:63-68.

Williams, J.A., K.S. Hathcock, D. Klug, Y. Harada, B. Choudhury, J.P. Allison, R. Abe, and R.J. Hodes. 2005. Regulated costimulation in the thymus is critical for T cell development: dysregulated CD28 costimulation can bypass the pre-TCR checkpoint. *J Immunol* 175:4199-4207.

Xing, S., F. Li, Z. Zeng, Y. Zhao, S. Yu, Q. Shan, Y. Li, F.C. Phillips, P.K. Maina, H.H. Qi, C. Liu, J. Zhu, R.M. Pope, C.A. Musselman, C. Zeng, W. Peng, and H.H. Xue. 2016. Tcf1 and Lef1 transcription factors establish CD8 T cell identity through intrinsic HDAC activity. *Nat Immunol*

Xu, K., W.Y. Yang, G.K. Nanayakkara, Y. Shao, F. Yang, W. Hu, E.T. Choi, H. Wang, and X. Yang. 2018. GATA3, HDAC6, and BCL6 Regulate FOXP3+ Treg Plasticity and Determine Treg Conversion into Either Novel Antigen-Presenting Cell-Like Treg or Th1-Treg. *Frontiers in immunology* 9:45.

Yu, Q., B. Erman, J.H. Park, L. Feigenbaum, and A. Singer. 2004. IL-7 receptor signals inhibit expression of transcription factors TCF-1, LEF-1, and RORgammat: impact on thymocyte development. *J Exp Med* 200:797-803.

Yu, S., X. Zhou, F.C. Steinke, C. Liu, S.C. Chen, O. Zagorodna, X. Jing, Y. Yokota, D.K. Meyerholz, C.G. Mullighan, C.M. Knudson, D.M. Zhao, and H.H. Xue. 2012. The TCF-1 and LEF-1 transcription factors have cooperative and opposing roles in T cell development and malignancy. *Immunity* 37:813-826.

Zhang, M., C. Hu, N. Moses, J. Haakenson, S. Xiang, D. Quan, B. Fang, Z. Yang, W. Bai, G. Bepler, G.M. Li, and X.M. Zhang. 2019. HDAC6 regulates DNA damage response via deacetylating MLH1. *J Biol Chem* 294:5813-5826.

Zhang, X.-H., M. Qin, H.-P. Wu, M.Y. Khamis, Y.-H. Li, L.-Y. Ma, and H.-M. Liu. 2021. A Review of Progress in Histone Deacetylase 6 Inhibitors Research: Structural Specificity and Functional Diversity. *Journal of medicinal chemistry* 64:1362-1391.

Zhang, Y., S. Kwon, T. Yamaguchi, F. Cubizolles, S. Rousseaux, M. Kneissel, C. Cao, N. Li, H.L. Cheng, K. Chua, D. Lombard, A. Mizeracki, G. Matthias, F.W. Alt, S. Khochbin, and P. Matthias. 2008. Mice lacking histone deacetylase 6 have hyperacetylated tubulin but are viable and develop normally. *Mol Cell Biol* 28:1688-1701.

Zhao, X., Q. Shan, and H.-H. Xue. 2021. TCF1 in T cell immunity: a broadened frontier. *Nature Reviews Immunology*

Figure 1.

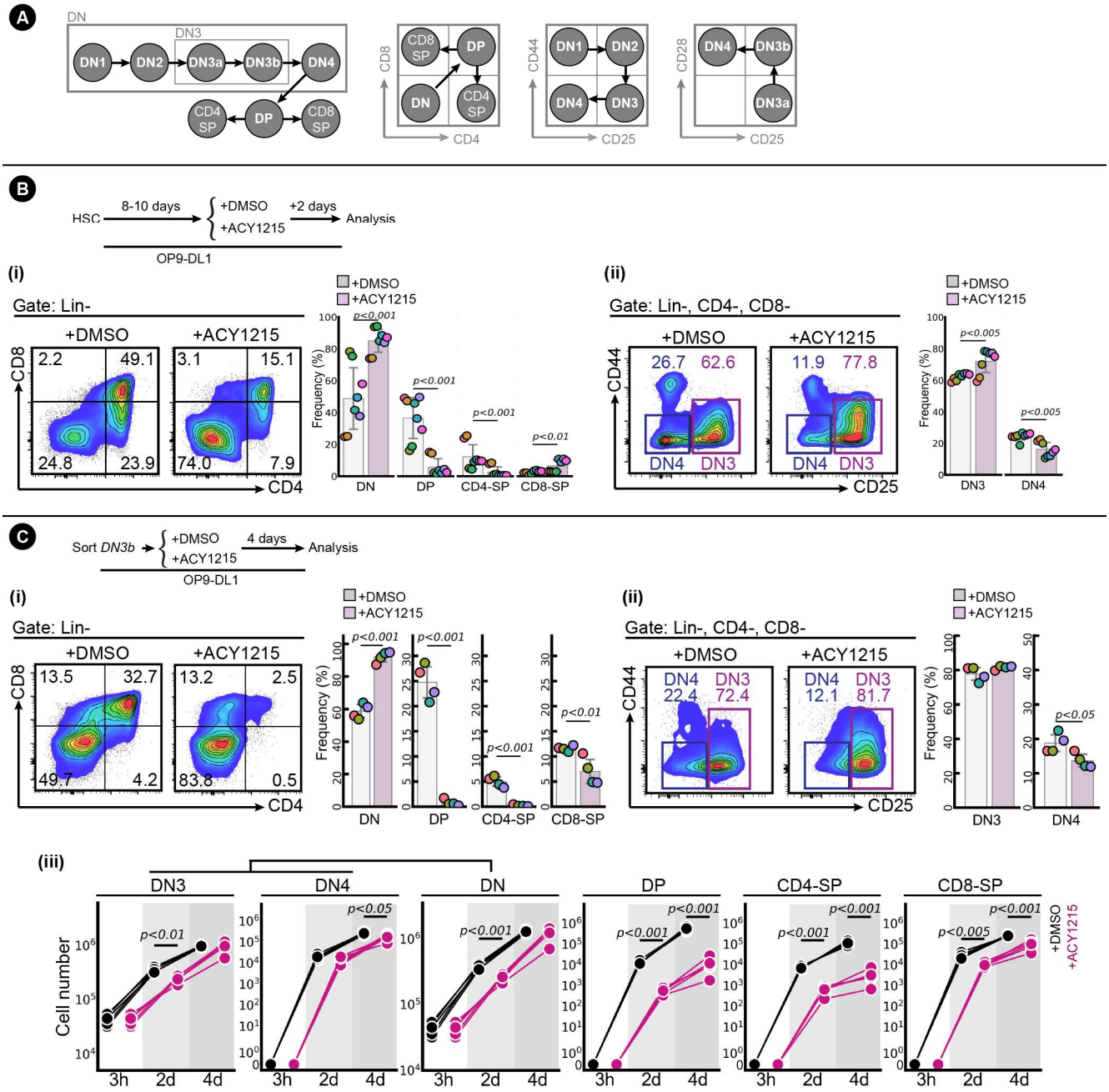
A
DN
DN3
DN1
DN2
DN3a
DN3b
DN4
CD4 SP
DP
CD8 SP
CD8
CD4
CD44
CD25
CD28
B
HSC
8-10 days
+DMSO
+ACY1215
+2 days
Analysis
OP9-DL1
(i)
Gate: Lin-
+DMSO
+ACY1215
Frequency (%)
DN
DP
CD4-SP
CD8-SP
(ii)
Gate: Lin-, CD4-, CD8-
DN4
DN3
C
Sort DN3b
4 days
(iii)
Cell number
3h
2d
4d

Figure 2.

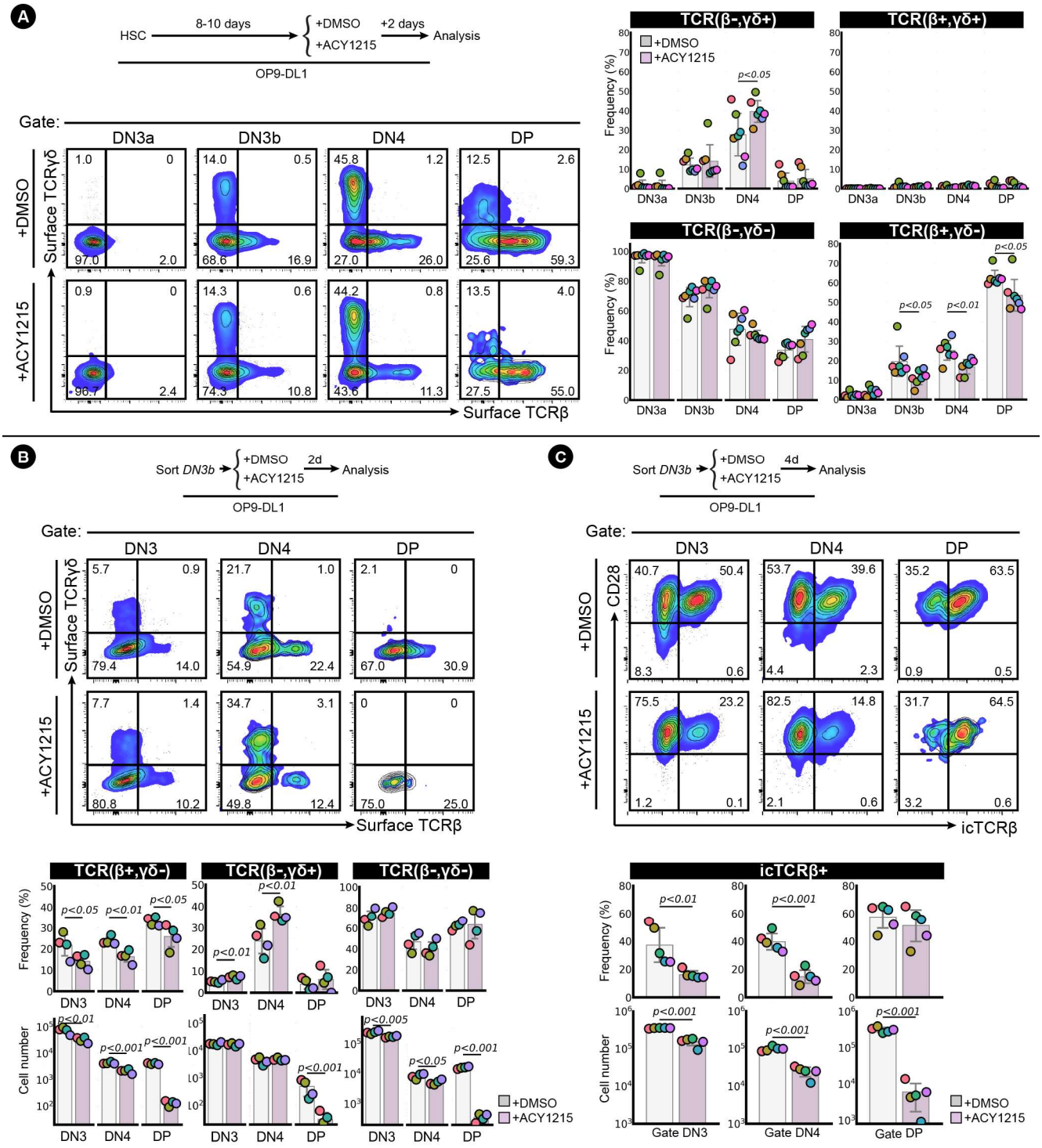
A
HSC
8-10 days
+DMSO
+ACY1215
+2 days
Analysis
OP9-DL1
Gate:
DN3a
DN3b
DN4
DP
+DMSO
+ACY1215
Surface TCRγδ
Surface TCRβ
TCR(β-,γδ+)
TCR(β+,γδ+)
TCR(β-,γδ-)
TCR(β+,γδ-)
Frequency (%)
p<0.05
p<0.01
B
Sort DN3b
2d
DN3
DN4
DP
Cell number
C
4d
CD28
icTCRβ
icTCRβ+
Gate DN3
Gate DN4
Gate DP

Figure 3.

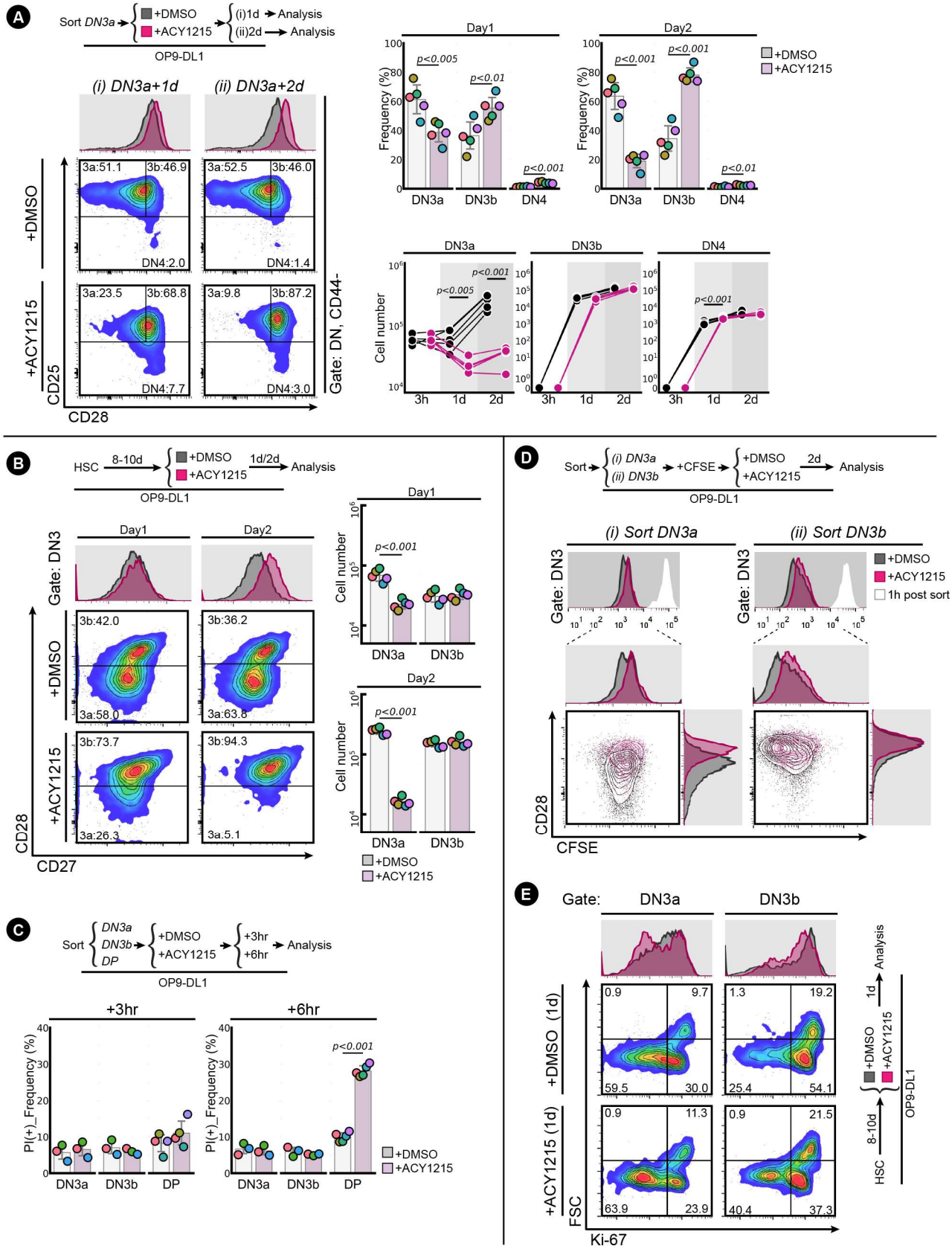
A
Sort DN3a
+DMSO
+ACY1215
(i)1d Analysis
(ii)2d Analysis
OP9-DL1
(i) DN3a+1d
(ii) DN3a+2d
3a:51.1
3b:46.9
DN4:2.0
3a:52.5
3b:46.0
DN4:1.4
3a:23.5
3b:68.8
DN4:7.7
3a:9.8
3b:87.2
DN4:3.0
CD25
CD28
Gate: DN, CD44-
Day1
Day2
Frequency (%)
p<0.005
p<0.01
p<0.001
DN3a
DN3b
DN4
Cell number
3h
1d
2d
B
HSC
8-10d
1d/2d
Gate: DN3
3b:42.0
3a:58.0
3b:36.2
3a:63.8
3b:73.7
3a:26.3
3b:94.3
3a.5.1
CD27
C
Sort
DN3a
DN3b
DP
+3hr
+6hr
PI(+)_Frequency (%)
D
(i) DN3a
(ii) DN3b
+CFSE
2d
(i) Sort DN3a
(ii) Sort DN3b
1h post sort
CFSE
E
Gate:
0.9
9.7
59.5
30.0
1.3
19.2
25.4
54.1
11.3
63.9
23.9
21.5
40.4
37.3
FSC
Ki-67
Analysis

Figure 4.

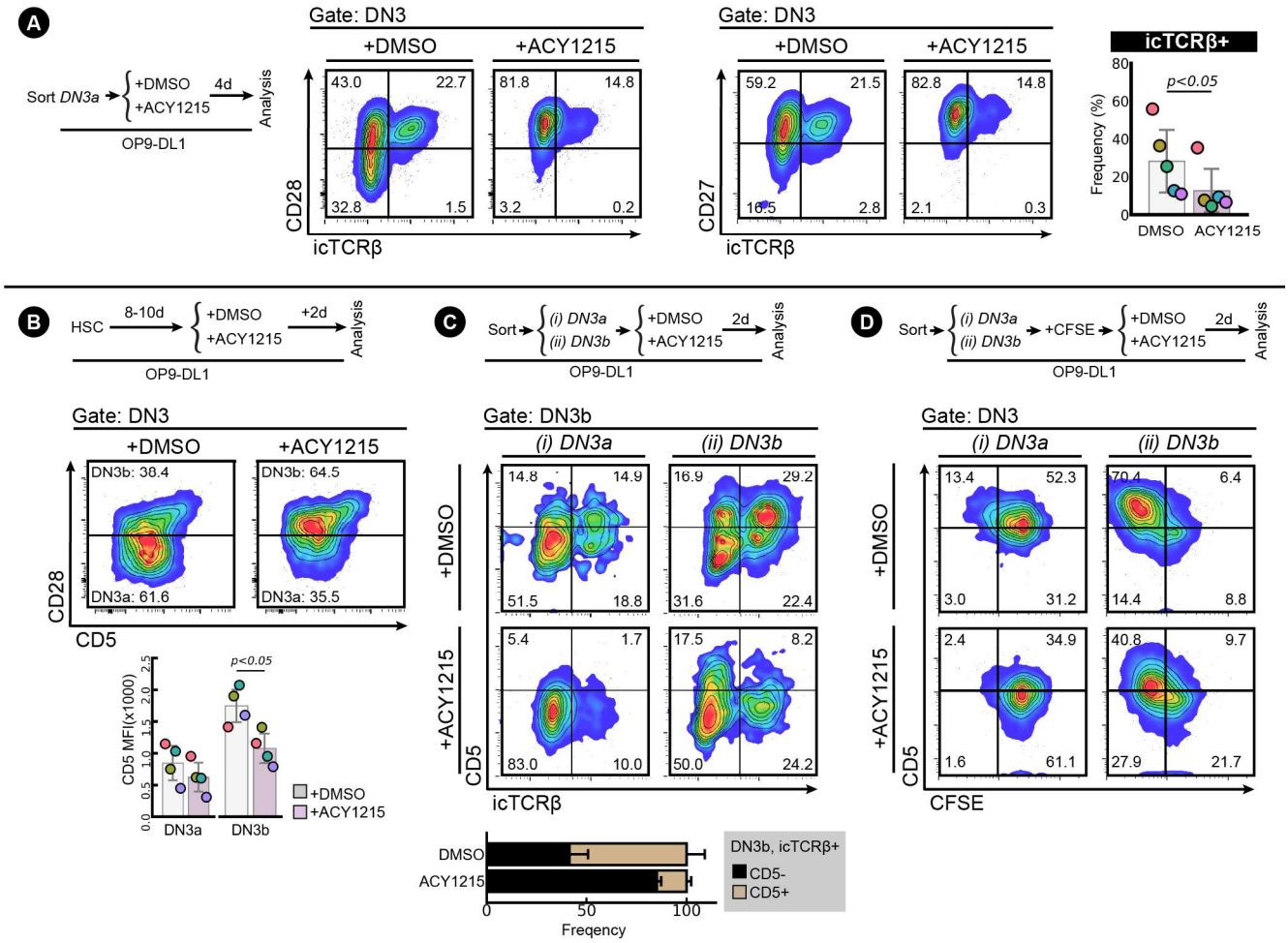
A
Sort DN3a
+DMSO
+ACY1215
4d
Analysis
OP9-DL1
Gate: DN3
+DMSO
+ACY1215
CD28
icTCRβ
43.0
22.7
32.8
1.5
81.8
14.8
3.2
0.2
CD27
59.2
21.5
16.5
2.8
82.8
14.8
2.1
0.3
icTCRβ+
p<0.05
Frequency (%)
DMSO
ACY1215
B
HSC
8-10d
+2d
C
Sort
(i) DN3a
(ii) DN3b
D
+CFSE
Gate: DN3b
CD5
DN3b: 38.4
DN3a: 61.6
DN3b: 64.5
DN3a: 35.5
CD5 MFI(x1000)
DN3a
DN3b
14.8
14.9
51.5
18.8
16.9
29.2
31.6
22.4
5.4
1.7
83.0
10.0
17.5
8.2
50.0
24.2
13.4
52.3
3.0
31.2
70.4
6.4
14.4
8.8
2.4
34.9
1.6
61.1
40.8
9.7
27.9
21.7
CFSE
Freqency
DN3b, icTCRβ+
CD5-
CD5+

Figure 5.

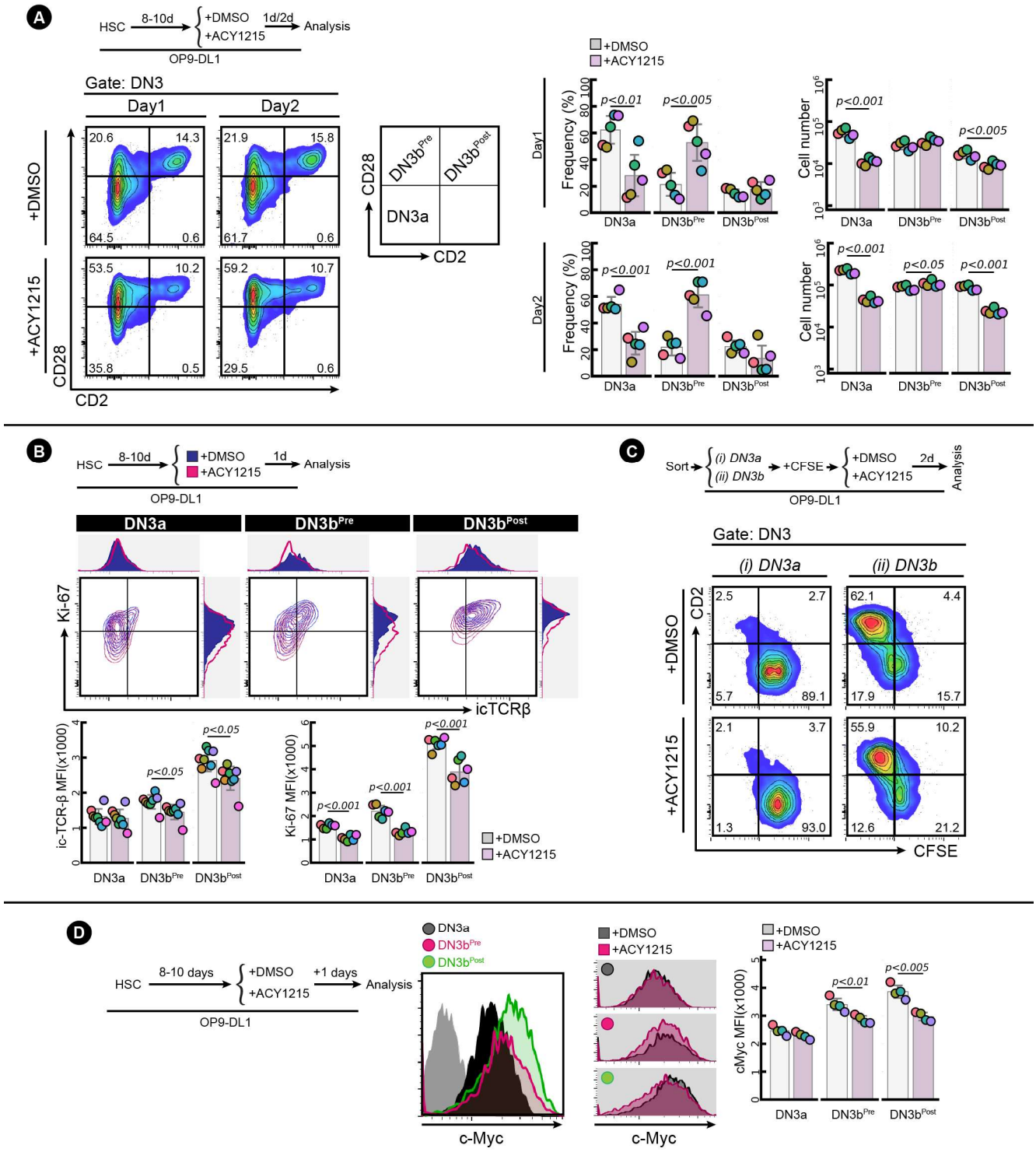
A
HSC
8-10d
+DMSO
+ACY1215
1d/2d
Analysis
OP9-DL1
Gate: DN3
Day1
Day2
+DMSO
+ACY1215
CD28
CD2
DN3b^Pre
DN3b^Post
DN3a
Frequency (%)
Cell number
p<0.01
p<0.005
p<0.001
p<0.05
B
1d
DN3a
DN3b^Pre
DN3b^Post
Ki-67
icTCRβ
ic-TCR-β MFI(x1000)
Ki-67 MFI(x1000)
C
Sort
(i) DN3a
(ii) DN3b
+CFSE
2d
Analysis
CFSE
D
8-10 days
+1 days
c-Myc
cMyc MFI(x1000)

Figure 6.

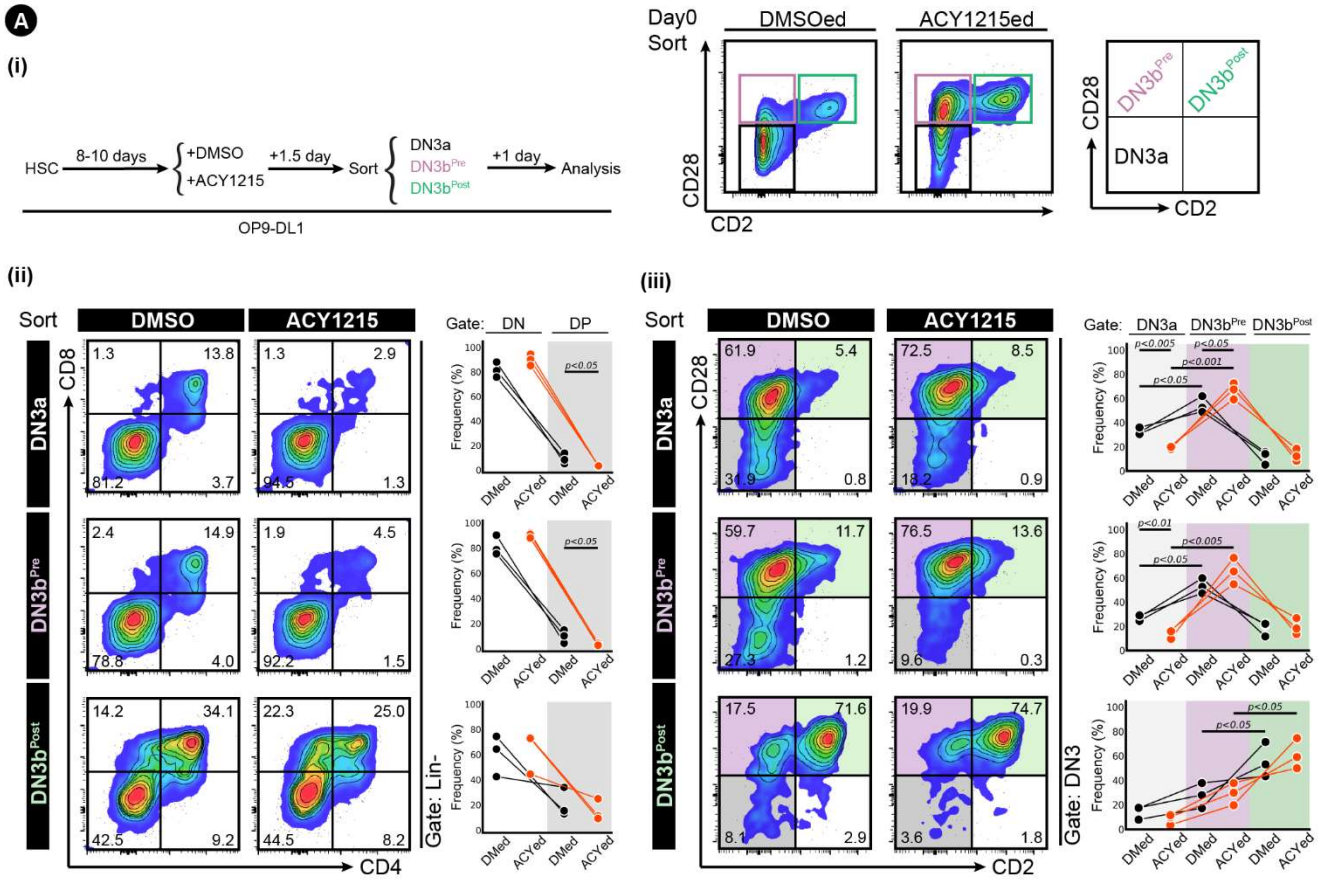
A
(i)
HSC
8-10 days
+DMSO
+ACY1215
+1.5 day
Sort
DN3a
DN3b^Pre
DN3b^Post
+1 day
Analysis
OP9-DL1
Day0
Sort
DMSOed
ACY1215ed
CD28
CD2
(ii)
Sort
DMSO
ACY1215
CD8
CD4
Gate: DN
DP
Gate: Lin-
Frequency (%)
DMed
ACYed
(iii)
Gate: DN3a
DN3b^Pre
DN3b^Post
Gate: DN3

Figure 7.

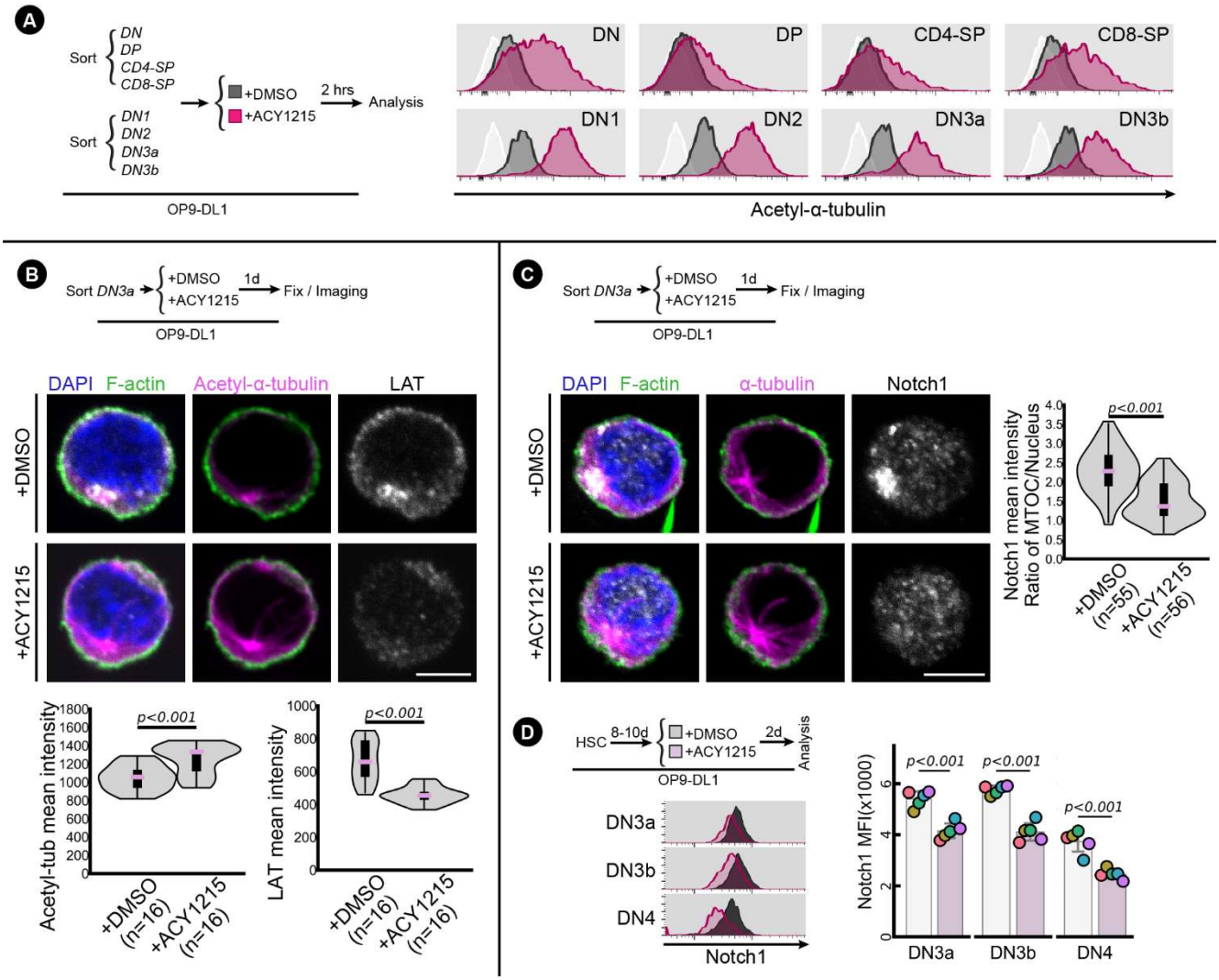
A
Sort
DN
DP
CD4-SP
CD8-SP
Sort
DN1
DN2
DN3a
DN3b
+DMSO
+ACY1215
2 hrs
Analysis
OP9-DL1
DN
DP
CD4-SP
CD8-SP
DN1
DN2
DN3a
DN3b
Acetyl-α-tubulin
B
Sort DN3a
+DMSO
+ACY1215
1d
Fix / Imaging
OP9-DL1
DAPI F-actin Acetyl-α-tubulin LAT
+DMSO
+ACY1215
Acetyl-tub mean intensity
p<0.001
+DMSO (n=16)
+ACY1215 (n=16)
LAT mean intensity
p<0.001
+DMSO (n=16)
+ACY1215 (n=16)
C
Sort DN3a
+DMSO
+ACY1215
1d
Fix / Imaging
OP9-DL1
DAPI F-actin α-tubulin Notch1
+DMSO
+ACY1215
Notch1 mean intensity Ratio of MTOC/Nucleus
p<0.001
+DMSO (n=55)
+ACY1215 (n=56)
D
HSC
8-10d
+DMSO
+ACY1215
2d
Analysis
OP9-DL1
DN3a
DN3b
DN4
Notch1
Notch1 MFI(x1000)
p<0.001
p<0.001
p<0.001
DN3a
DN3b
DN4

Figure 8.

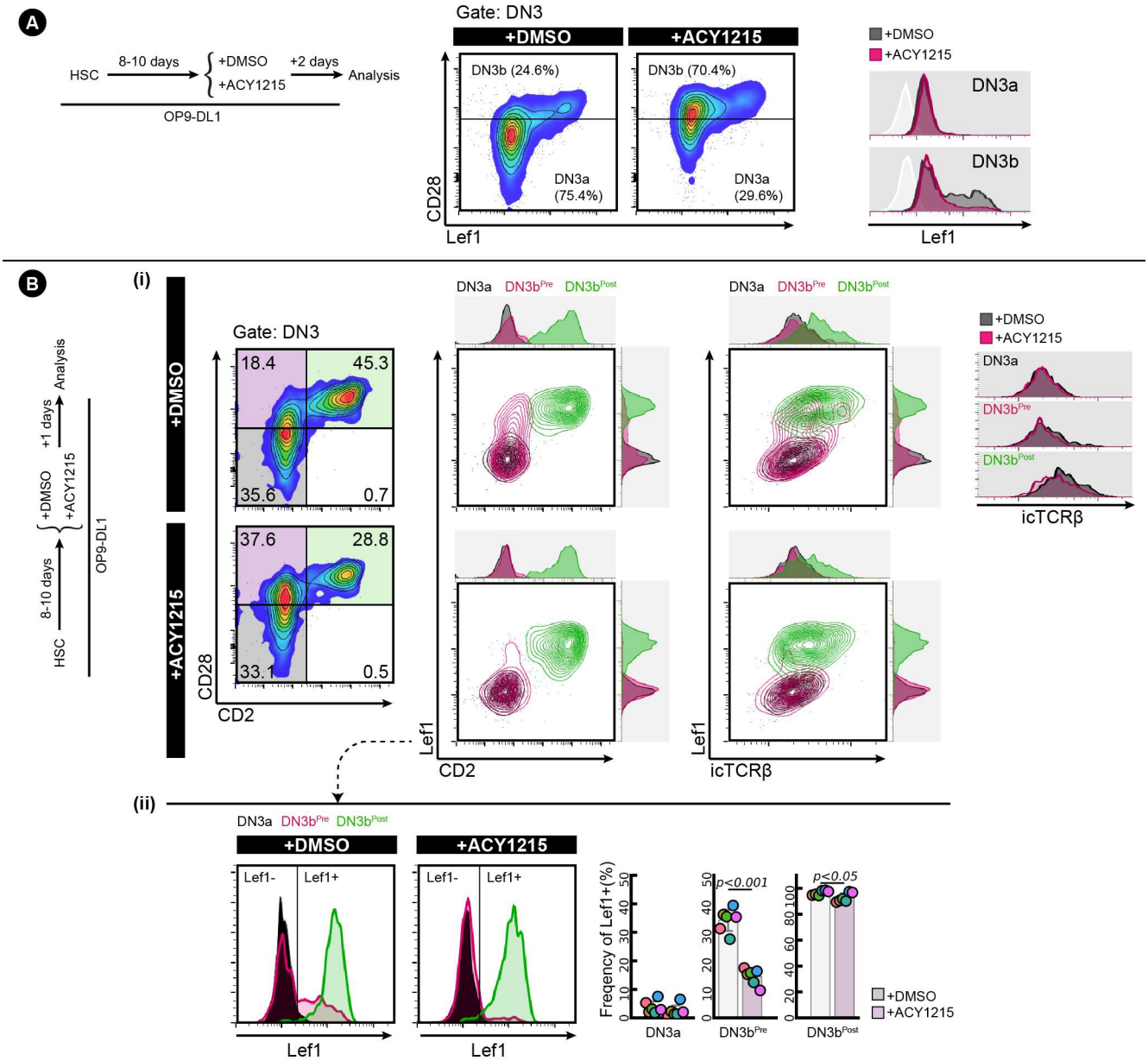

Chann et al. A histone deacetylase 6 inhibitor disrupts early αβ T cell development

Figure 9.

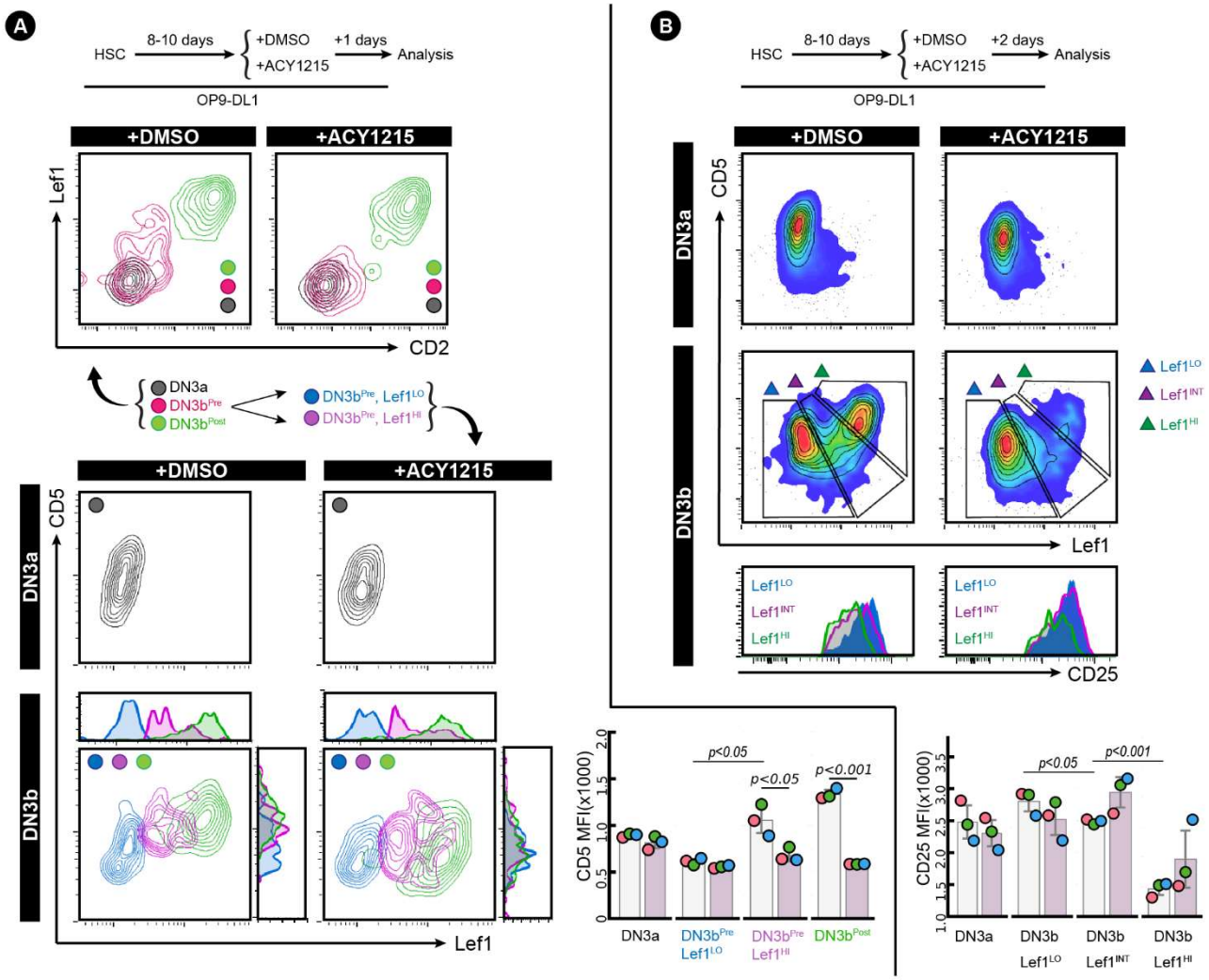
A
HSC
8-10 days
+DMSO
+ACY1215
+1 days
Analysis
OP9-DL1
+DMSO
+ACY1215
Lef1
CD2
DN3a
DN3b^Pre
DN3b^Post
DN3b^Pre, Lef1^LO
DN3b^Pre, Lef1^HI
CD5
DN3b
Lef1
B
+2 days
CD25
Lef1^LO
Lef1^INT
Lef1^HI
CD5 MFI(x1000)
CD25 MFI(x1000)
p<0.05
p<0.001
DN3a
DN3b^Pre Lef1^LO
DN3b^Pre Lef1^HI
DN3b^Post
DN3b Lef1^LO
DN3b Lef1^INT
DN3b Lef1^HI

Figure 10.

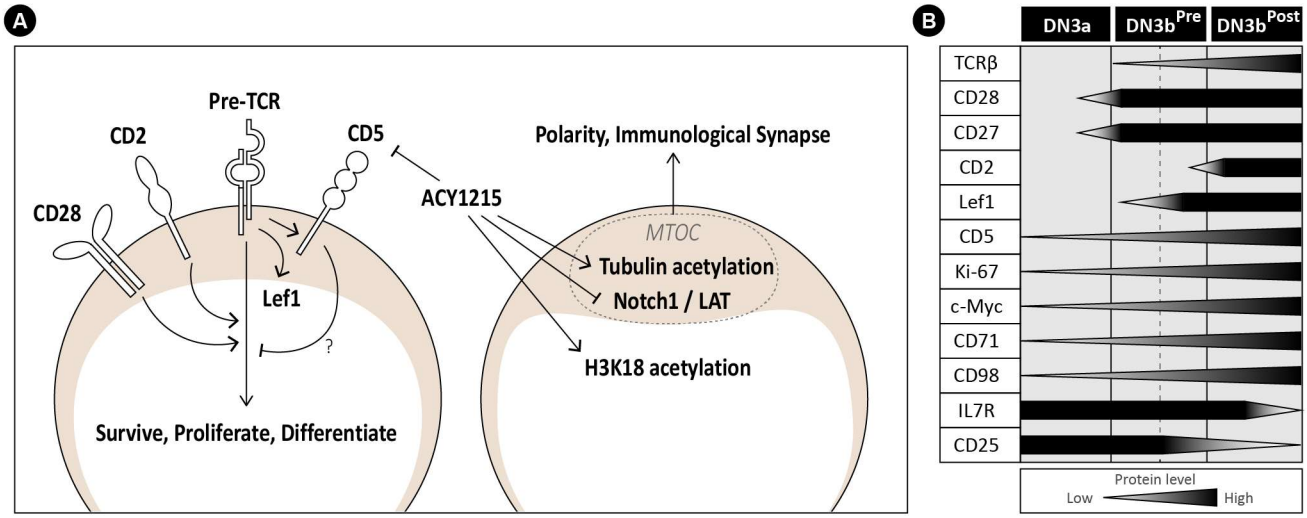
A
Pre-TCR
CD2
CD5
CD28
ACY1215
Polarity, Immunological Synapse
MTOC
Tubulin acetylation
Notch1 / LAT
Lef1
?
H3K18 acetylation
Survive, Proliferate, Differentiate
B
DN3a
DN3b Pre
DN3b Post
TCRβ
CD28
CD27
CD2
Lef1
CD5
Ki-67
c-Myc
CD71
CD98
IL7R
CD25
Protein level
Low
High

Supplementary Figure 1

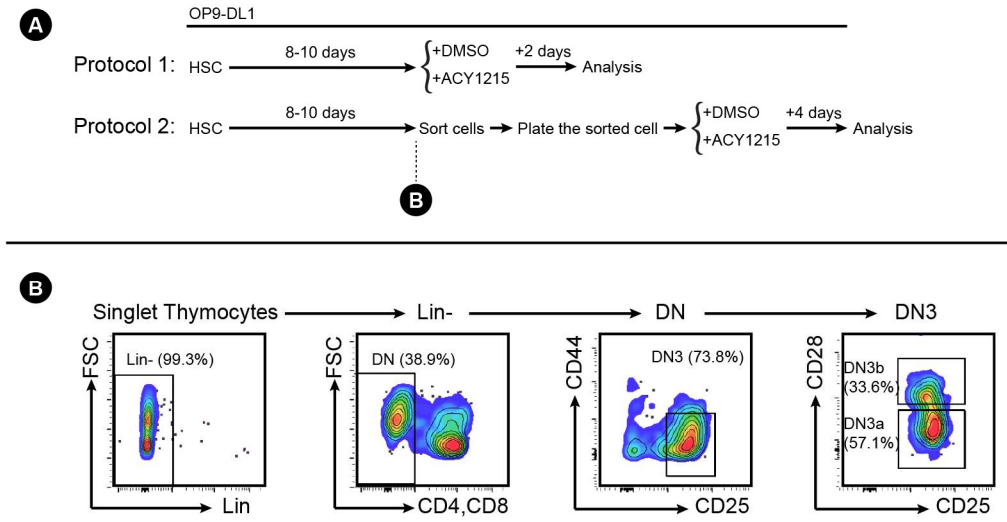

Supplementary Figure 2

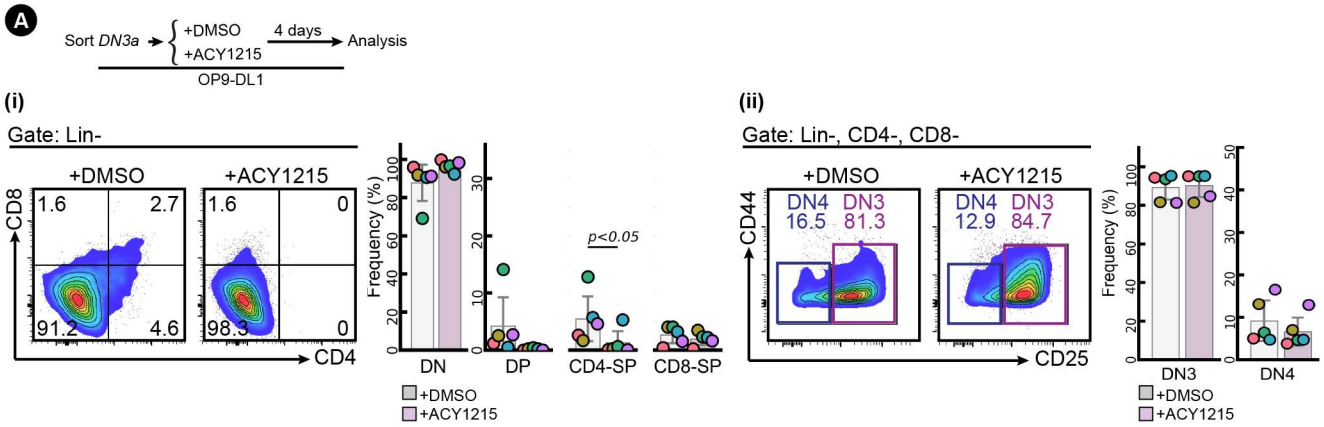

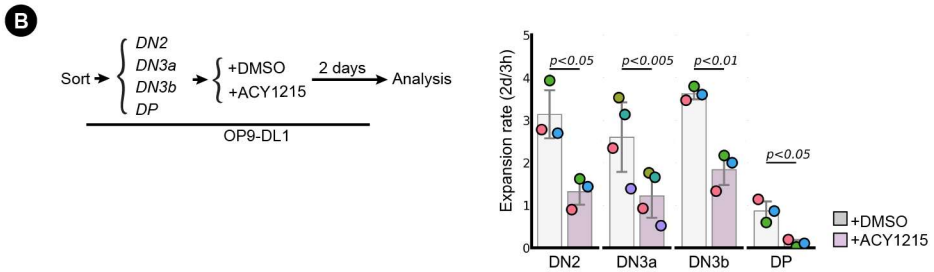

Supplementary Figure 3

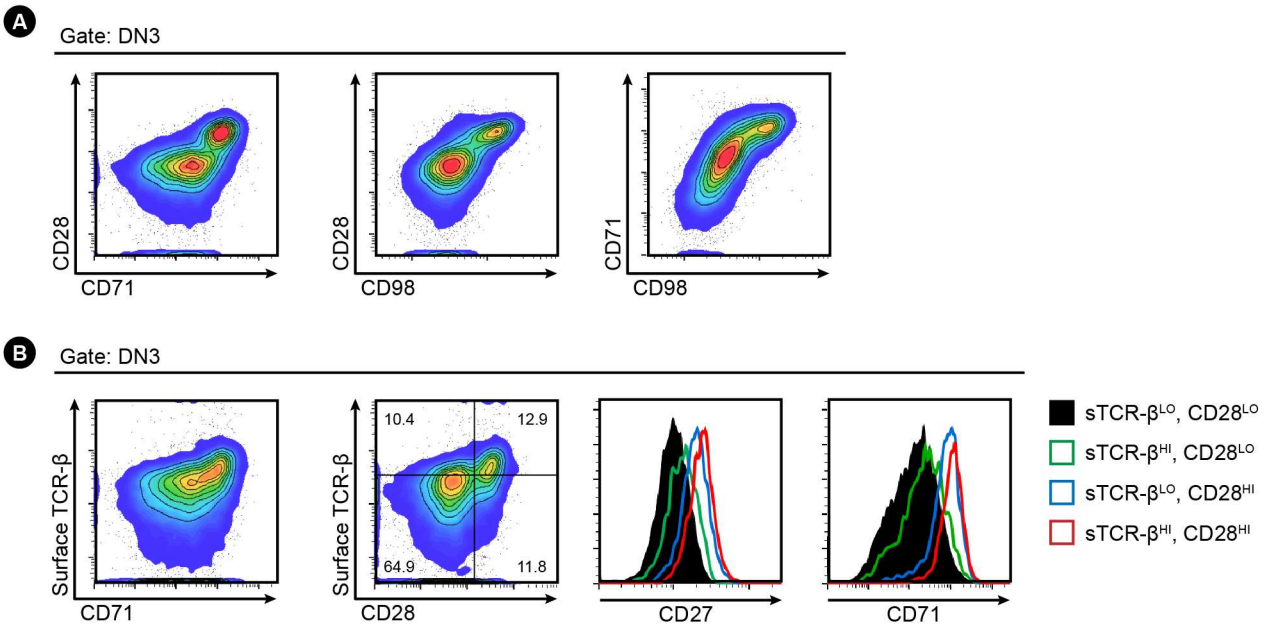

Supplementary Figure 4

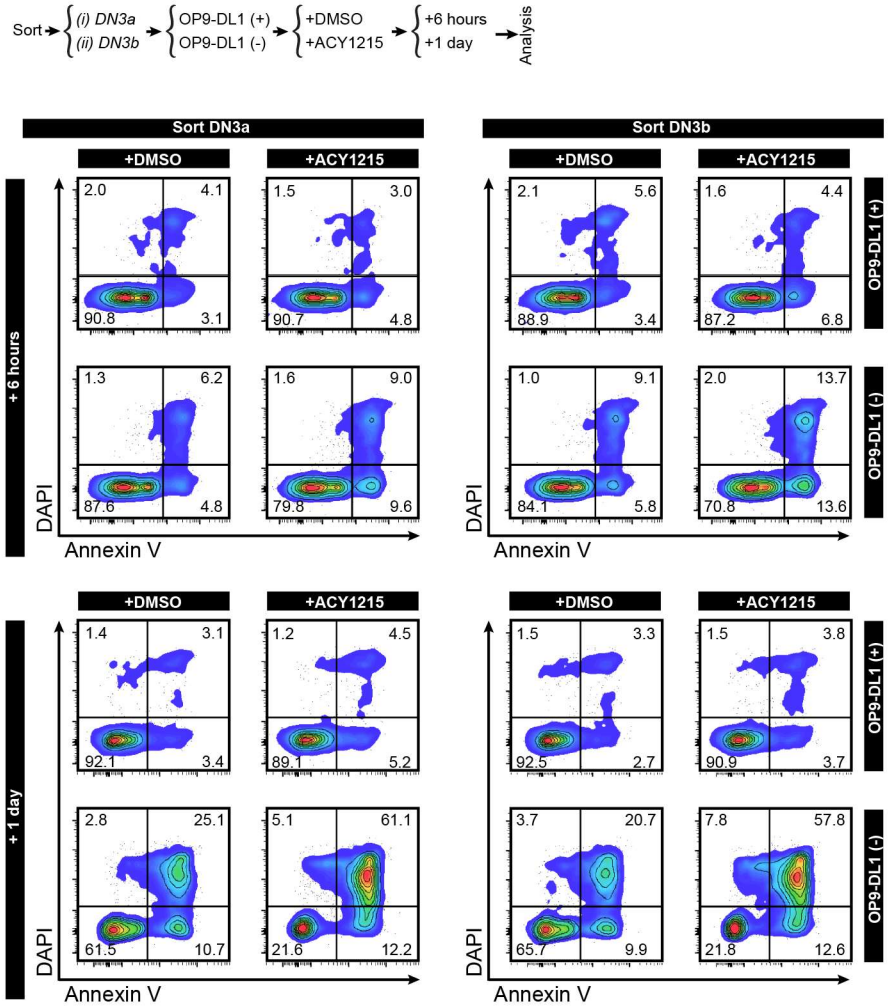

Supplementary Figure 5

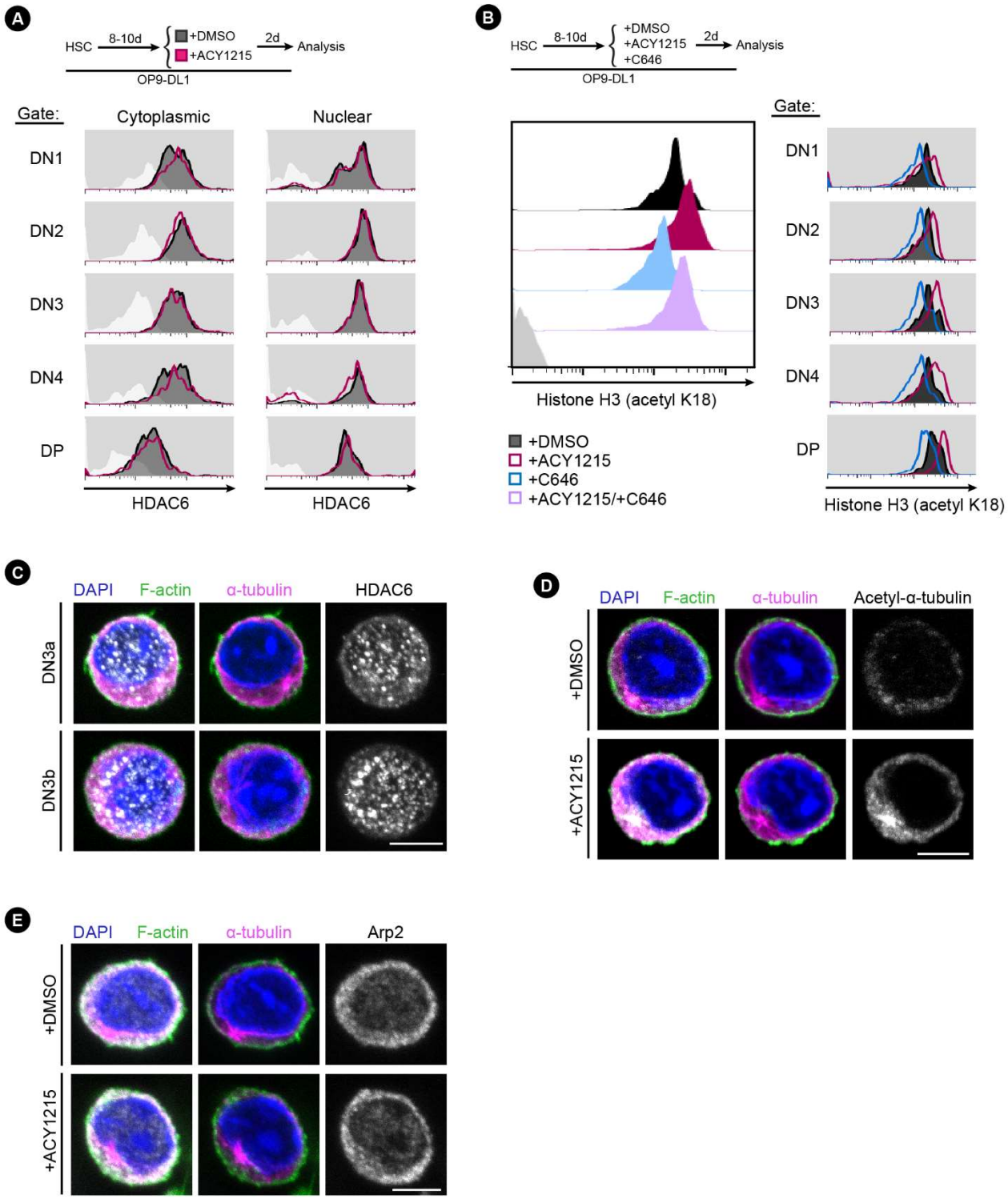

Supplementary Figure 6

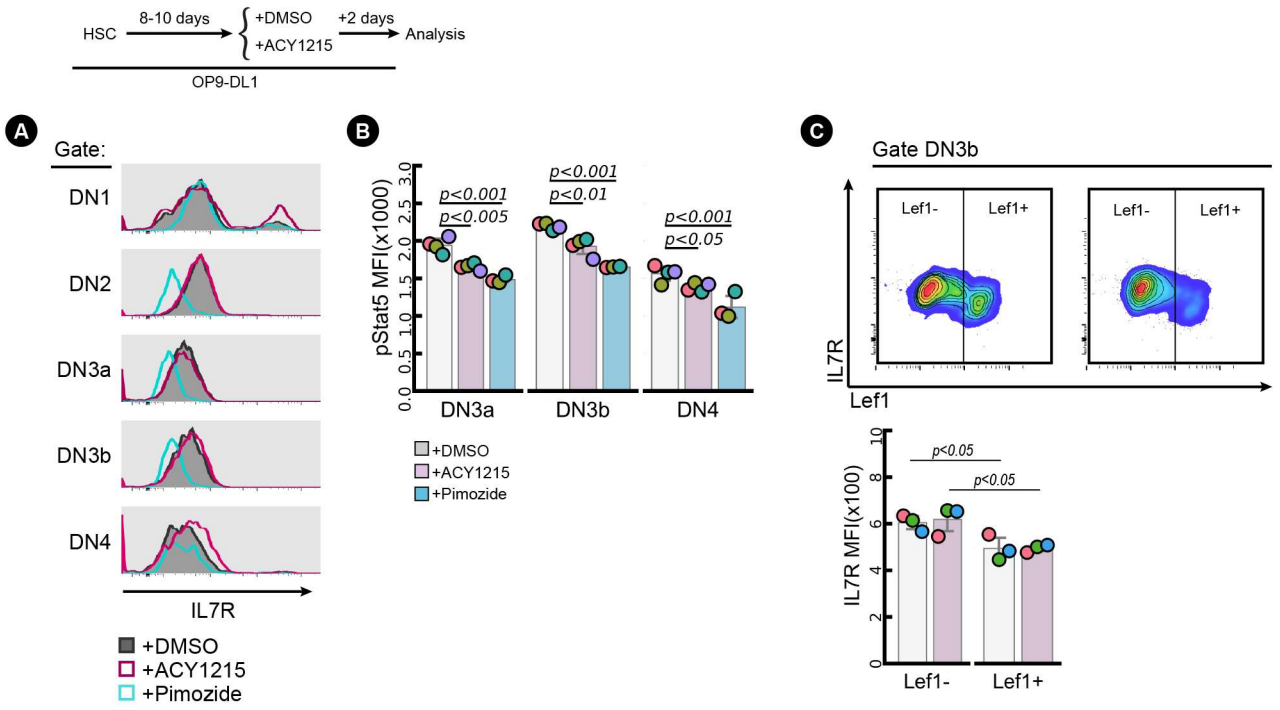

Supplementary Figure 7

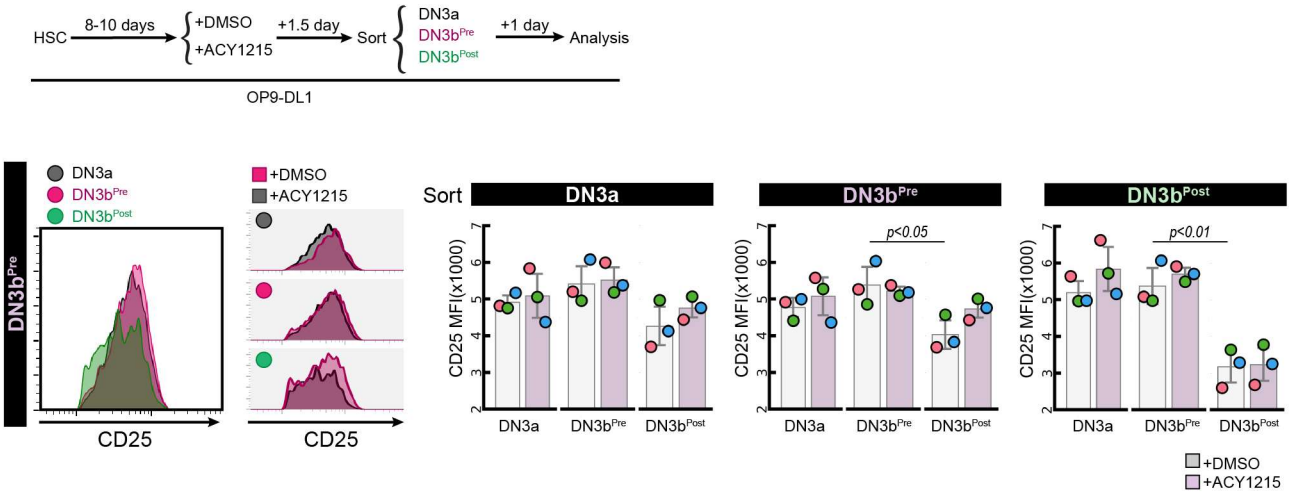
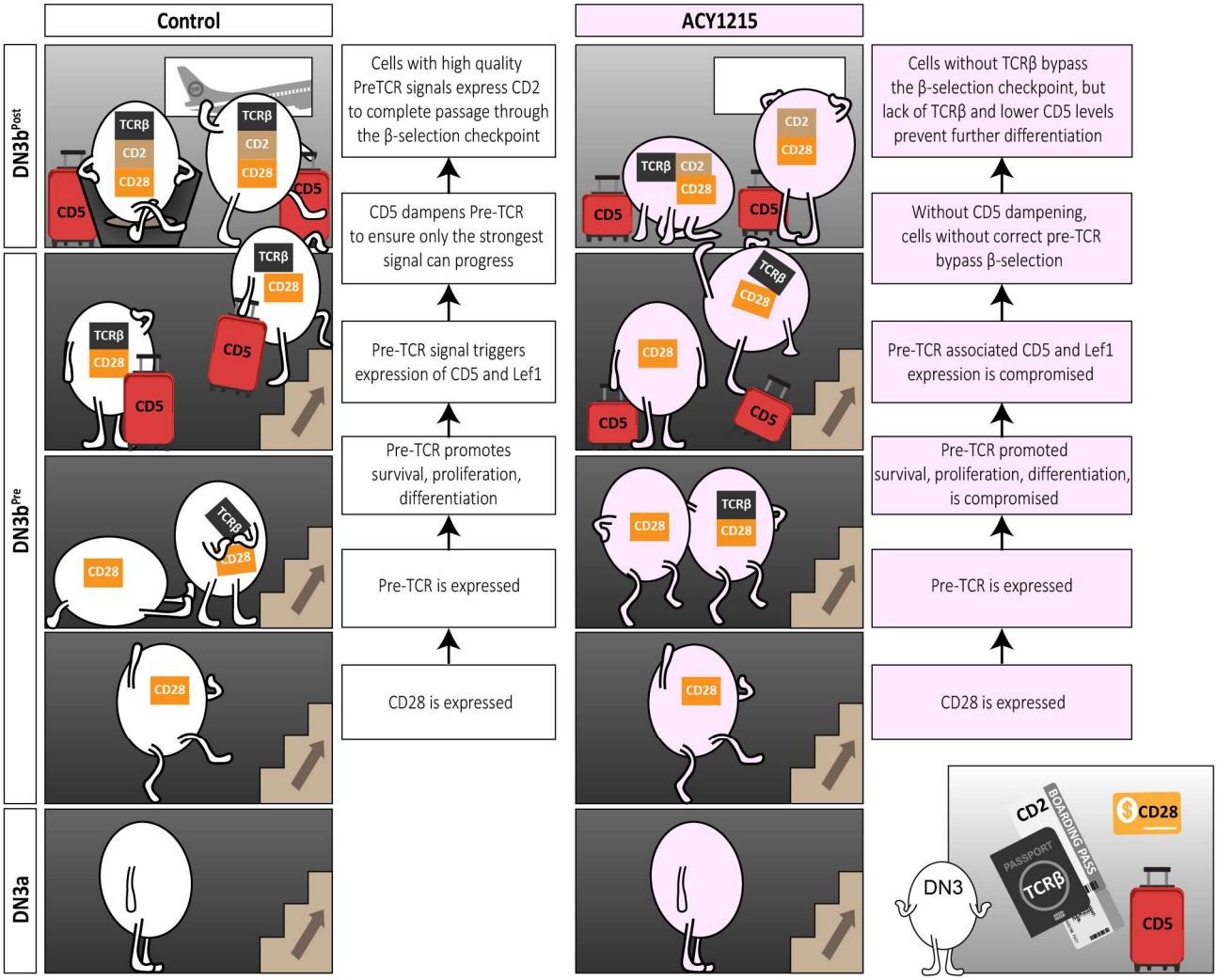
Supplementary Figure 8